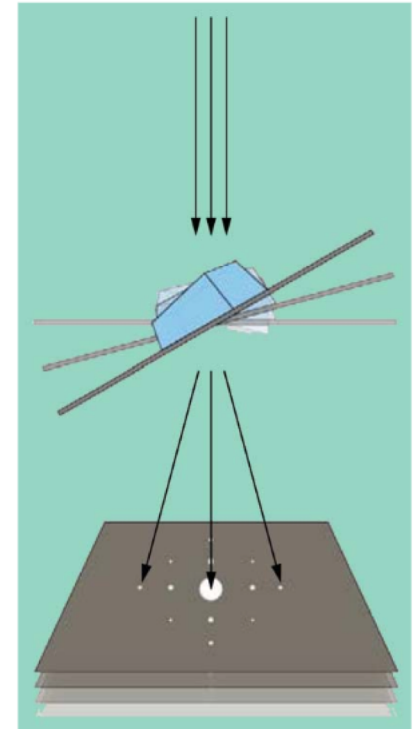


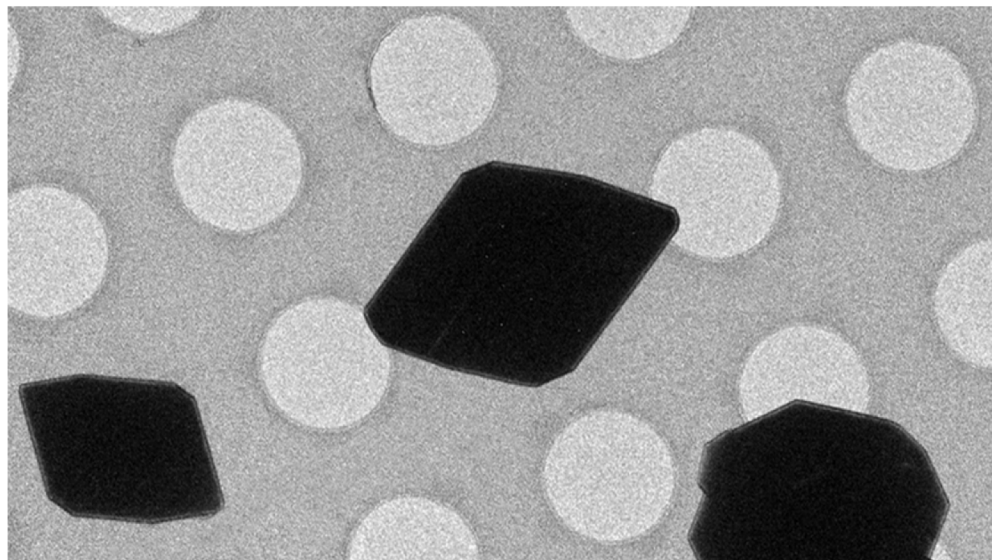
# MicroED

March 18, 2019



# Runner-up for Science's 2018 Breakthrough of the Year

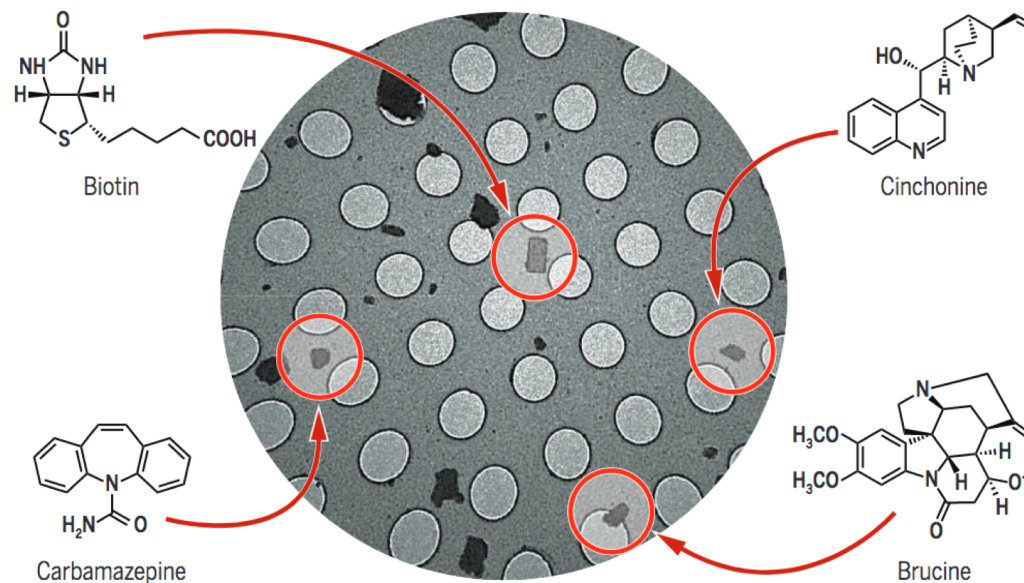
## Molecular structures made simple



Structures can now be gleaned from micrometer-size crystals (black), seen here on an electron microscope slide. (GONEN LAB)

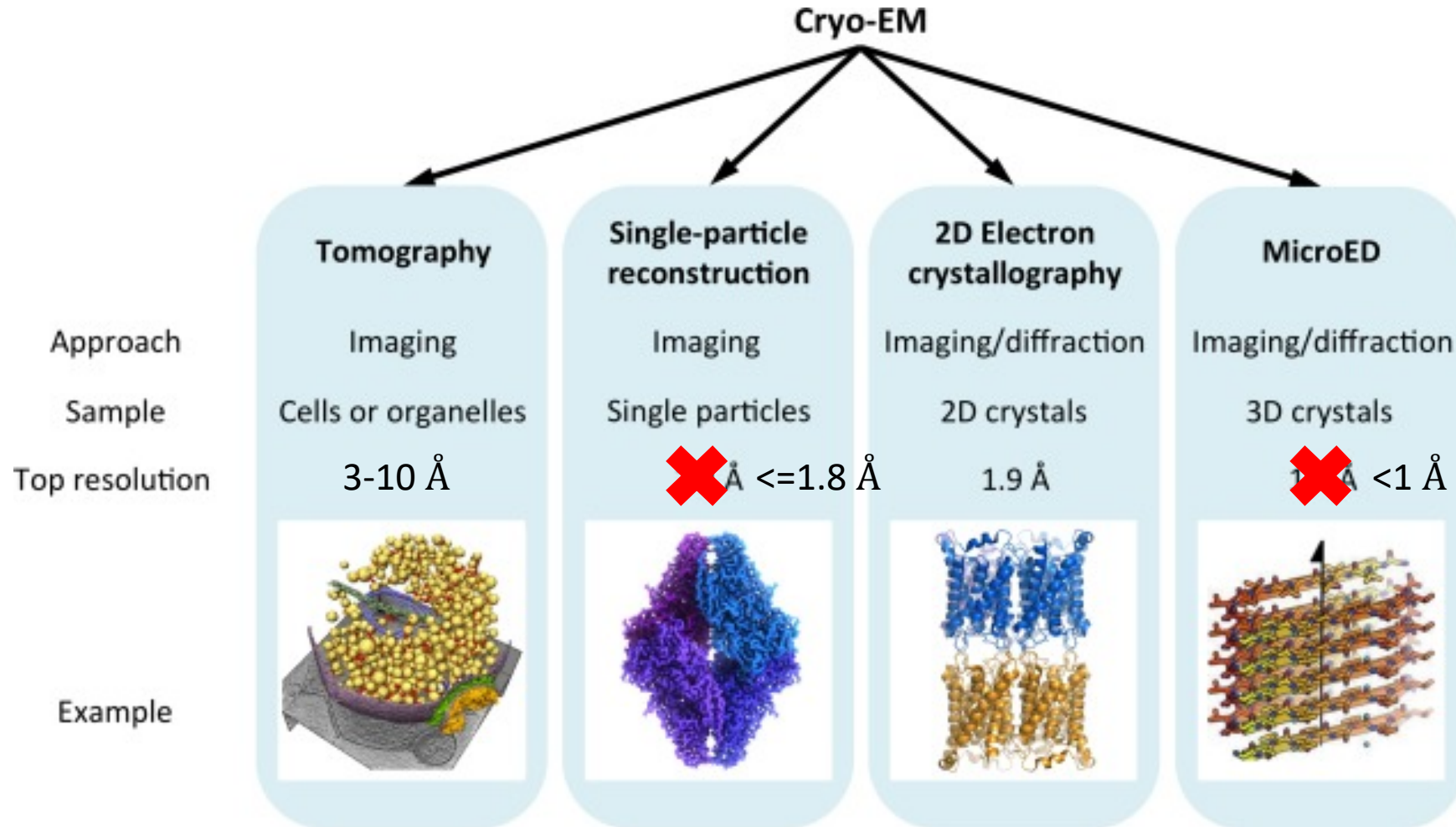
## Structures from a mix of microcrystals

A new technique identified structures of four compounds from tiny crystals on an electron microscope slide.

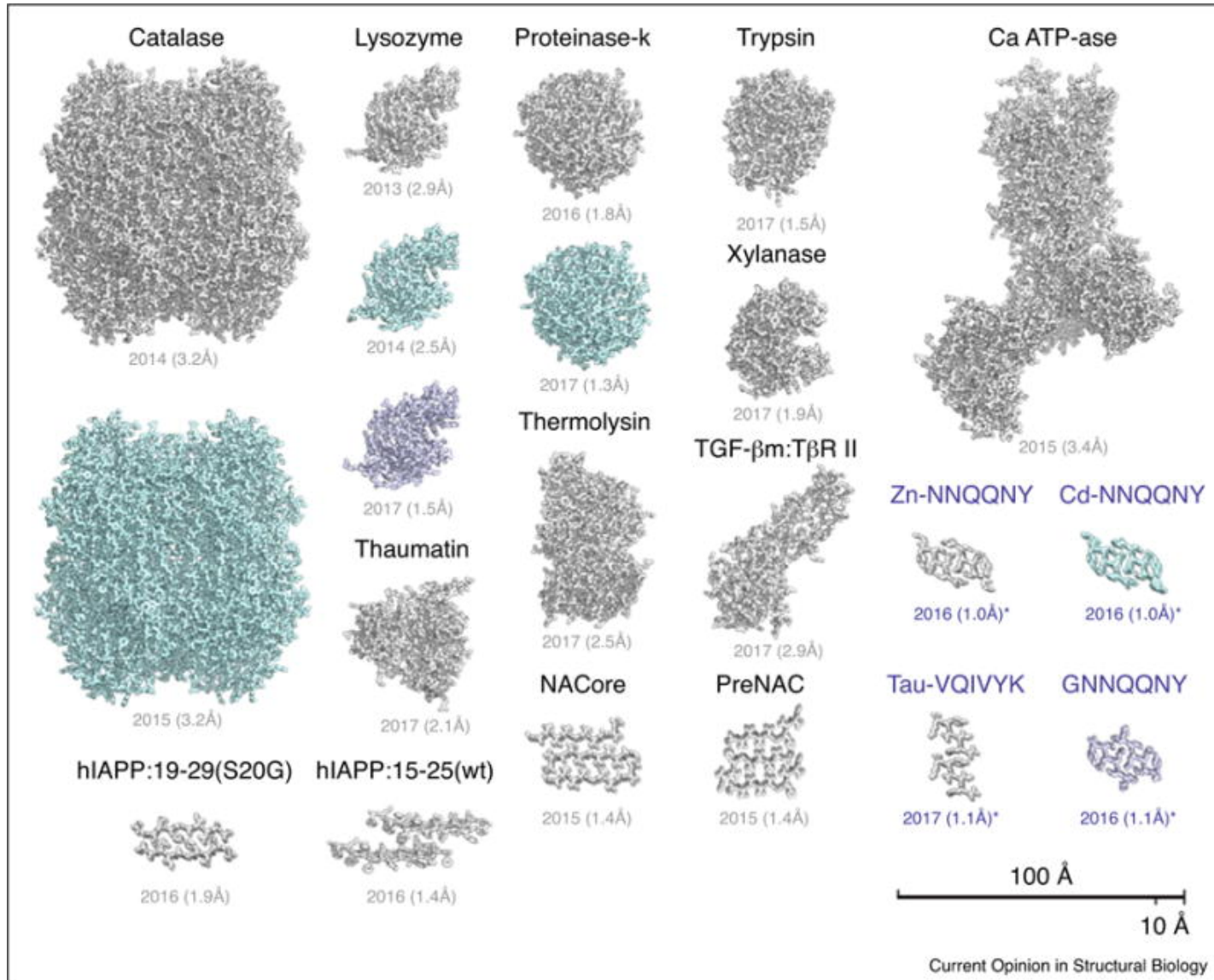




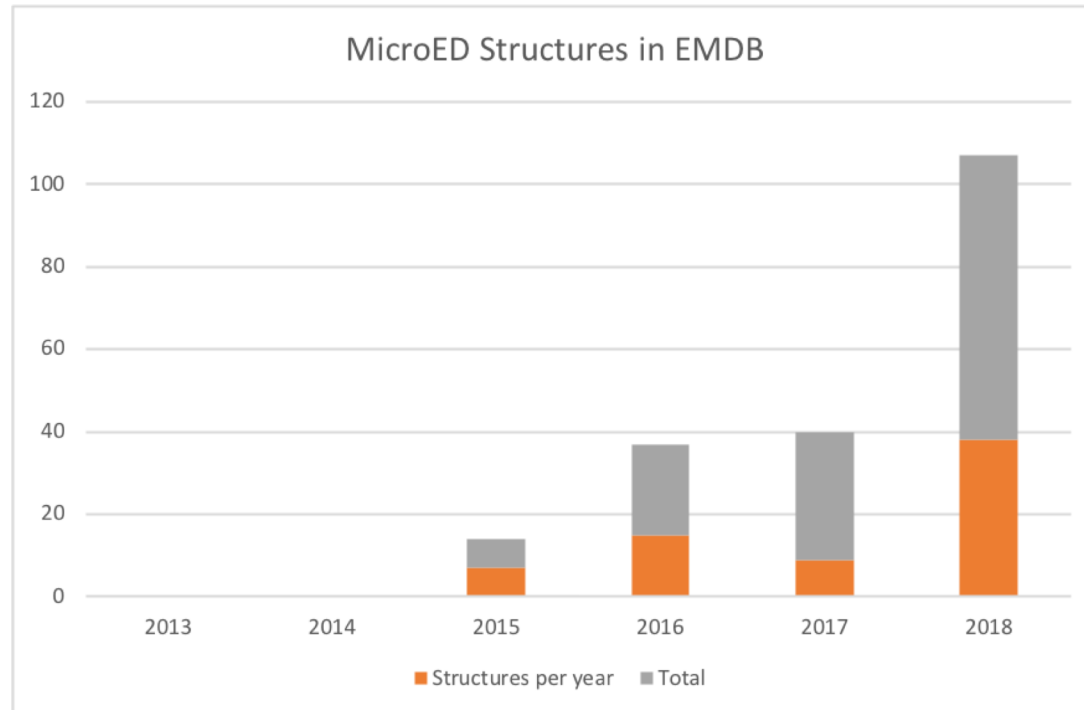
# Best Resolution from EM Techniques



# Structures Solved by MicroED



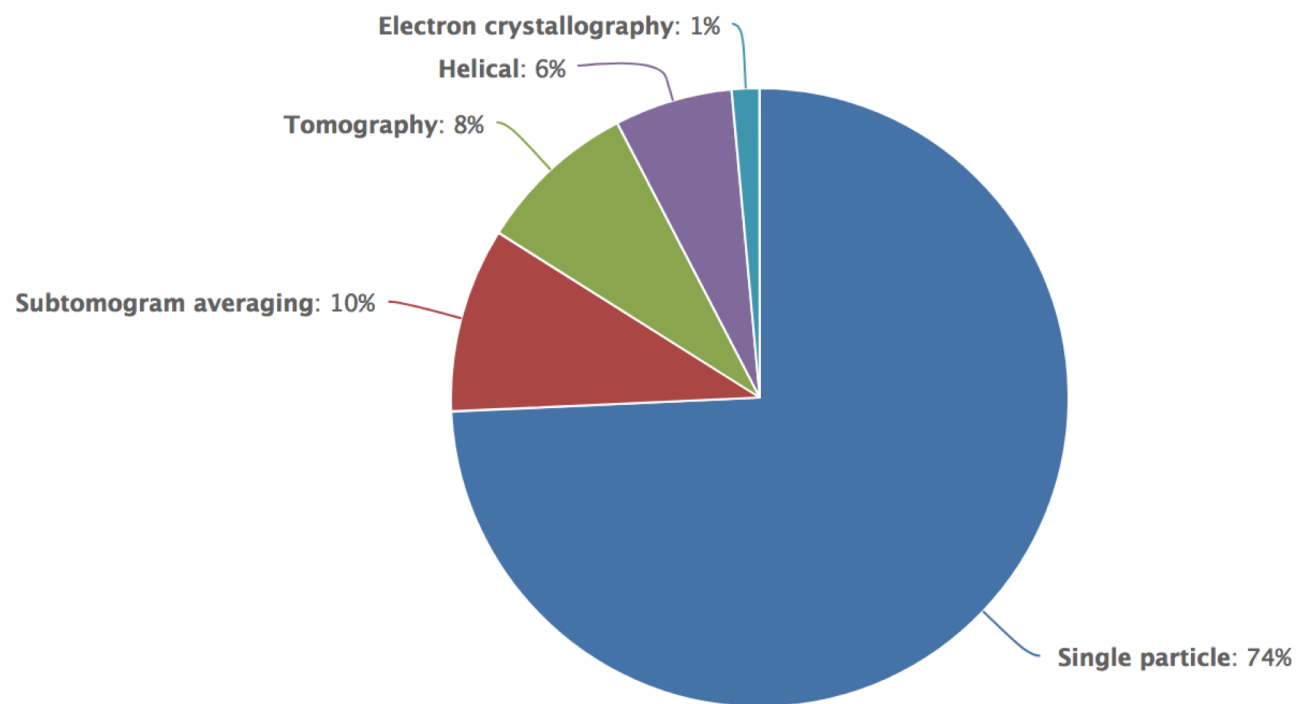
# Structures Solved by MicroED (EMDB search)



Year	Deposited Structures per year	Total Structures
2013	0	0
2014	0	0
2015	7	7
2016	15	22
2017	9	31
2018	38	69

# EMDB Statistics

Distribution of released maps (7780 in total) as a function of technique used



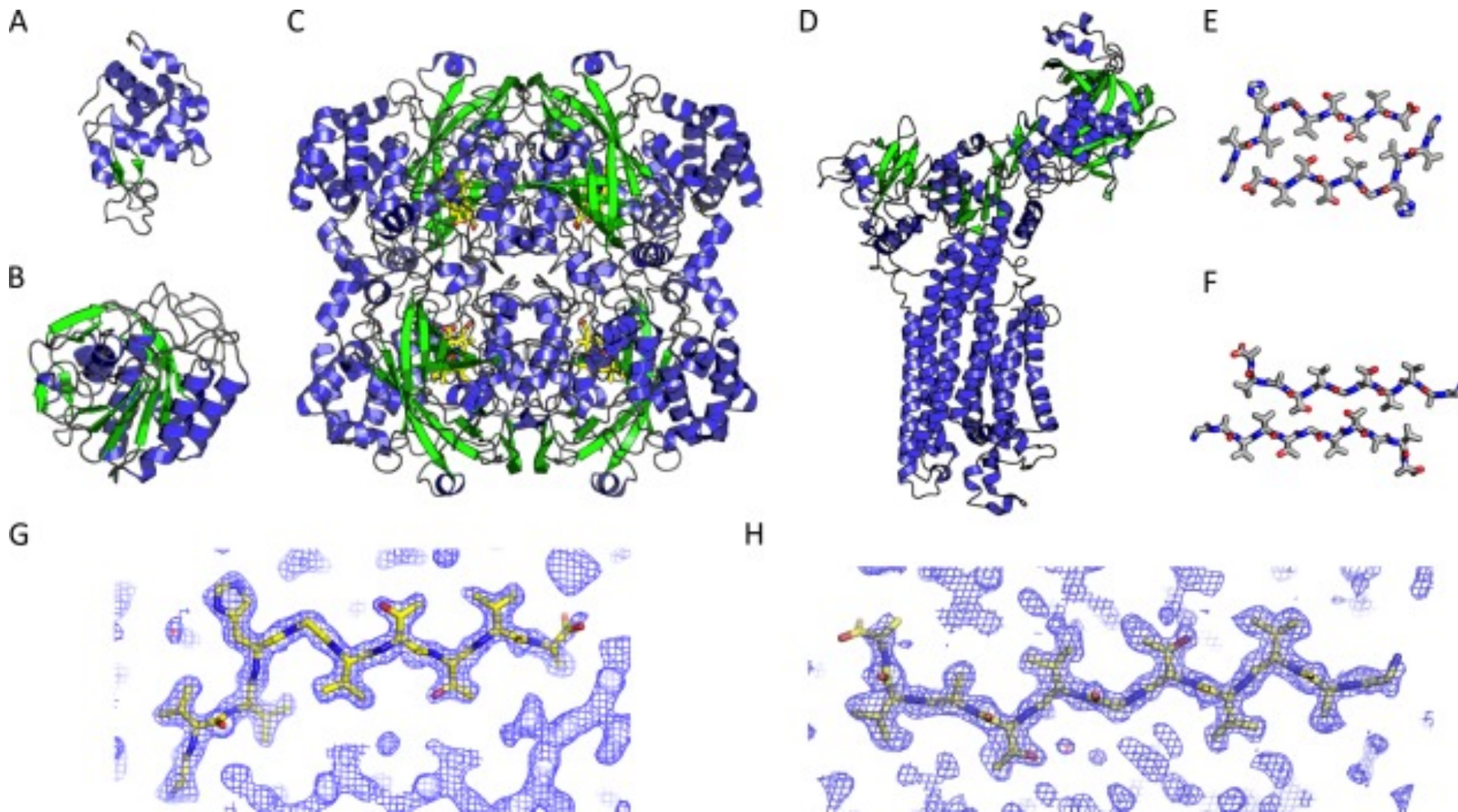
69/115 by MicroED  
32 of these <1 kDa

# Structures Solved by MicroED

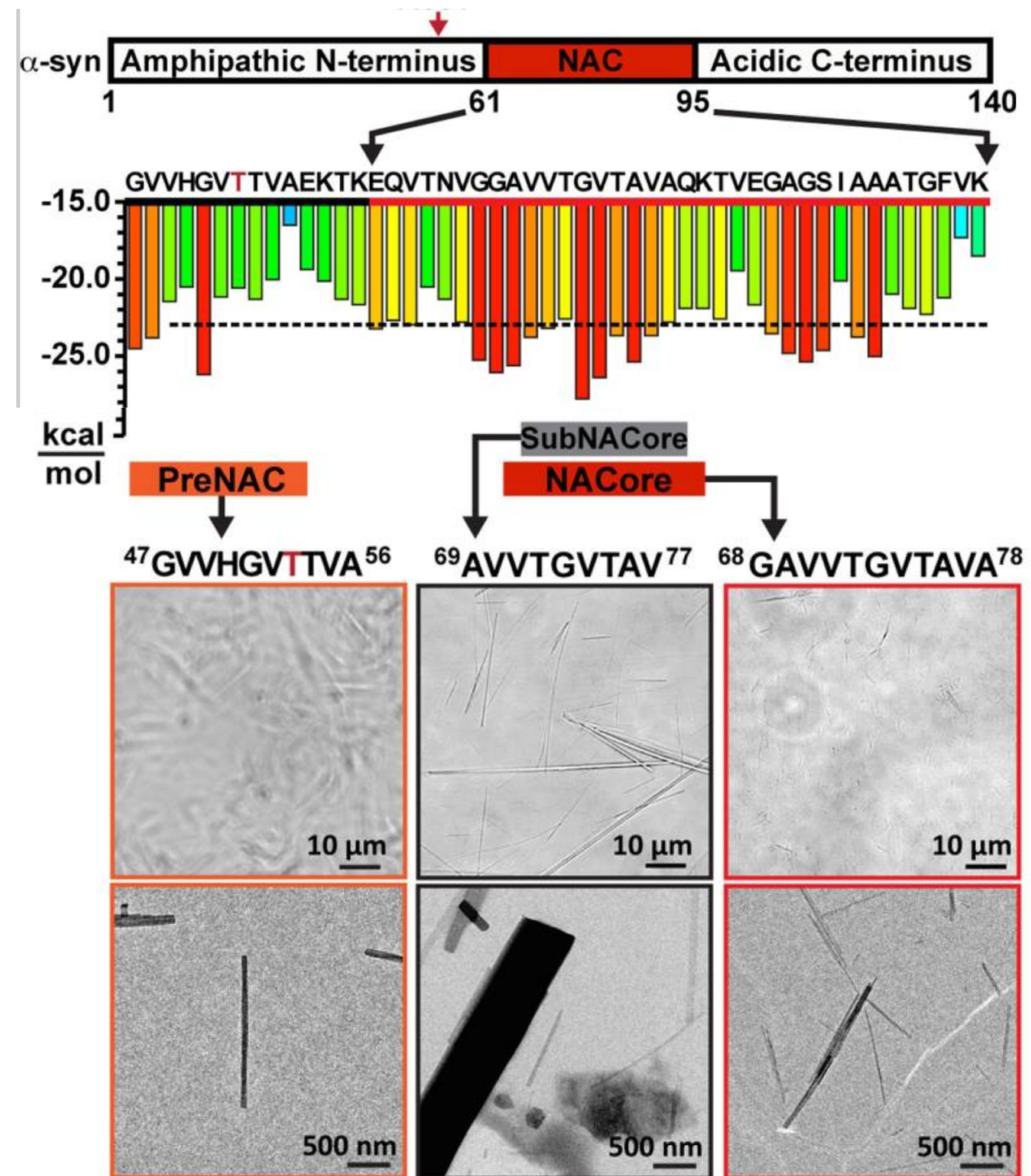
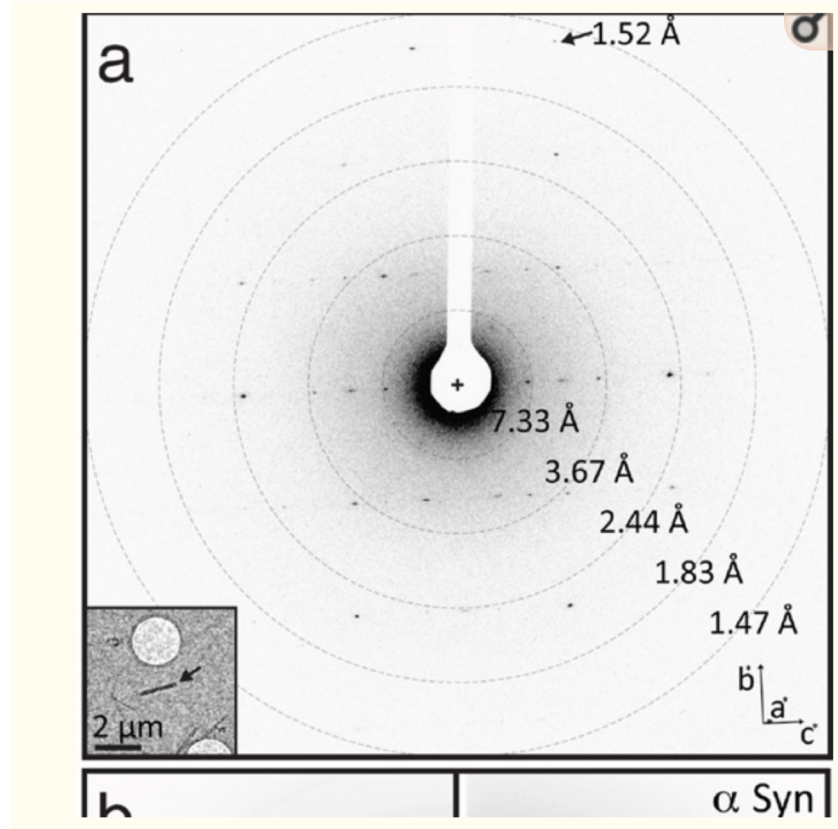
Sample	PDB code	R <sub>work</sub>   R <sub>free</sub> (%)	Ref	Phasing method	Res. (Å)	Space group	Cell dimensions a, b, c (Å)   α, β, γ (°)
Lysozyme	3J4G	25.5   27.8	[7••]	MR	2.9	P 4 <sub>3</sub> 2 <sub>1</sub> 2	77, 77, 37   90, 90, 90
Lysozyme	3J6K	22.0   25.5	[8••]	MR	2.5	P 4 <sub>3</sub> 2 <sub>1</sub> 2	76, 76, 37   90, 90, 90
Lysozyme	5K70	23.9   28.4	[36••]	MR	1.5	P 4 <sub>3</sub> 2 <sub>1</sub> 2	76, 76, 37   90, 90, 90
Catalase	3J7B	26.2   30.8	[10•]	MR	3.2	P 2 <sub>1</sub> 2 <sub>1</sub> 2 <sub>1</sub>	68, 172, 182   90, 90, 90
Catalase	3J7U	27.2   31.7	[11•]	MR	3.2	P 2 <sub>1</sub> 2 <sub>1</sub> 2 <sub>1</sub>	69, 174, 206   90, 90, 90
Ca-ATPase	3J7T	27.7   31.5	[11•]	MR	3.4	C 2	166, 64, 147   90, 98, 90
Proteinase K	519S	19.7   25.6	[9•]	MR	1.8	P 4 <sub>3</sub> 2 <sub>1</sub> 2	67, 67, 102   90, 90, 90
Proteinase K	5K7S	22.4   25.5	[36••]	MR	1.3	P 4 <sub>3</sub> 2 <sub>1</sub> 2	67.6, 67.6, 101.4   90, 90, 90
Thermolysin	5K7T	28.7   30.6	[36••]	MR	1.6	P 6 <sub>1</sub> 2 2	90.8, 90.8, 126   90, 90, 120
Trypsin	5K7R	24.8   28.1	[36••]	MR	1.5	P 2 <sub>1</sub> 2 <sub>1</sub> 2 <sub>1</sub>	53.1, 56.1, 64.4   90, 90, 90
Thaumatococcus	5K7Q	24.5   29.2	[36••]	MR	2.1	P 4 <sub>1</sub> 2 <sub>1</sub> 2	57.8, 57.8, 150   90, 90, 90
Xylanase	5K7P	22.1   26.2	[36••]	MR	1.9	P 2 <sub>1</sub> 2 <sub>1</sub> 2 <sub>1</sub>	49.1, 59, 70   90, 90, 90
TGFβ:TBRII	5TY4	29.2   32.8	[36••]	MR	2.9	P 2 <sub>1</sub> 2 <sub>1</sub> 2 <sub>1</sub>	41.5, 71.3, 79.5   90, 90, 90
NACore	4RIL	24.8   27.5	[14••]	MR	1.4	C 2	70.8, 4.8, 16.8   90, 106, 90
PreNAC	4ZNN	23.5   28.2	[14••]	MR	1.4	P 2 <sub>1</sub>	17.9, 4.7, 33   90, 94, 90
hIAPP 19-29 (S20G)	5KNZ	22.8   27.5	[35•]	MR	1.9	P 2 <sub>1</sub> 2 <sub>1</sub> 2 <sub>1</sub>	4.8, 18.6, 70.8   90, 90, 90
hIAPP 15-25 (WT)	5KO0	22.4   25.9	[35•]	MR	1.4	P 1	11.7, 18.2, 19.9   63, 89, 88
Tau (VQIVYK)	5K7N	21.0   22.4	[36••] <sup>a</sup>	DM	1.1	C 2	29.3, 4.97, 37.6   90, 112, 90
Sup35 (Zn-NNQQNY)	5K2E	15.6   19.4	[12••] <sup>a</sup>	DM	1.0	P 2 <sub>1</sub>	21.5, 4.9, 23.9   90, 104, 90
Sup35 (Cd-NNQQNY)	5K2F	22.0   24.2	[12••] <sup>a</sup>	DM	1.0	P 2 <sub>1</sub>	22.1, 4.9, 23.5   90, 104, 90
Sup35 (GNNQQNY-1)	5K2G	18.7   22.4	[12••] <sup>a</sup>	DM	1.1	P 2 <sub>1</sub>	22.9, 4.9, 24.2   90, 108, 90
Sup35 (GNNQQNY-2)	5K2H	17.7   18.6	[12••] <sup>a</sup>	DM	1.05	P 2 <sub>1</sub> 2 <sub>1</sub> 2 <sub>1</sub>	23.2, 4.9, 40.5   90, 90, 90



# Sample Structures

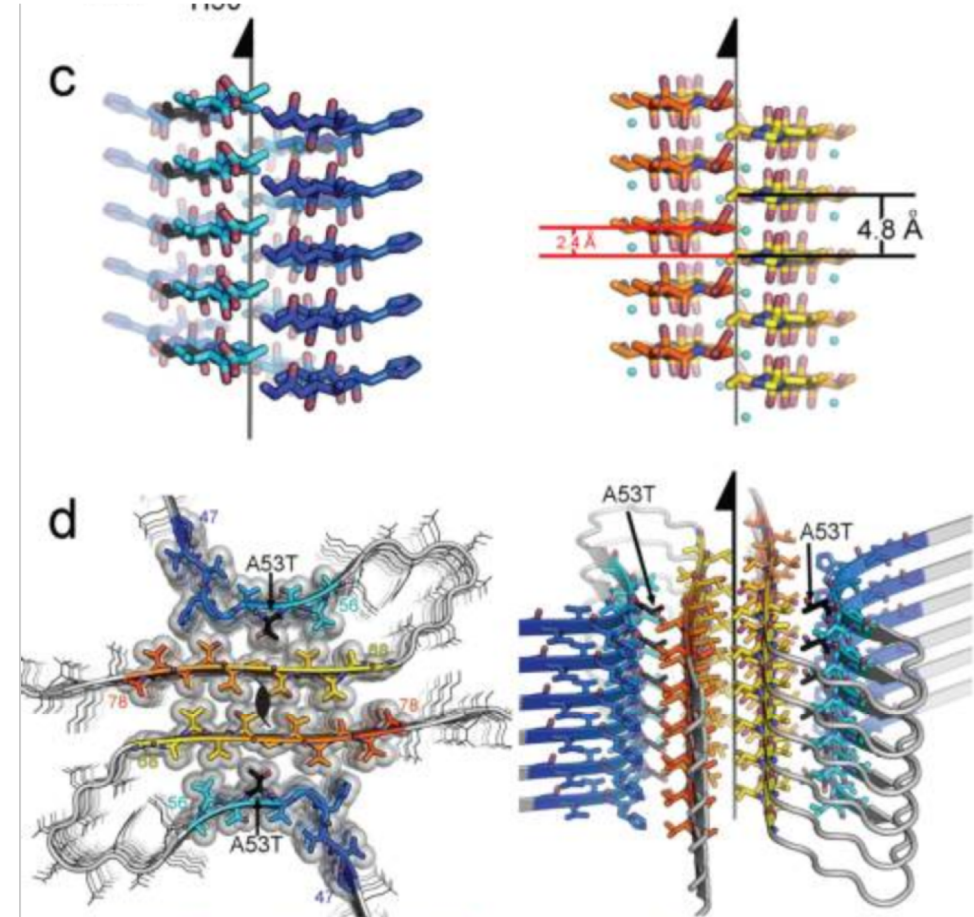
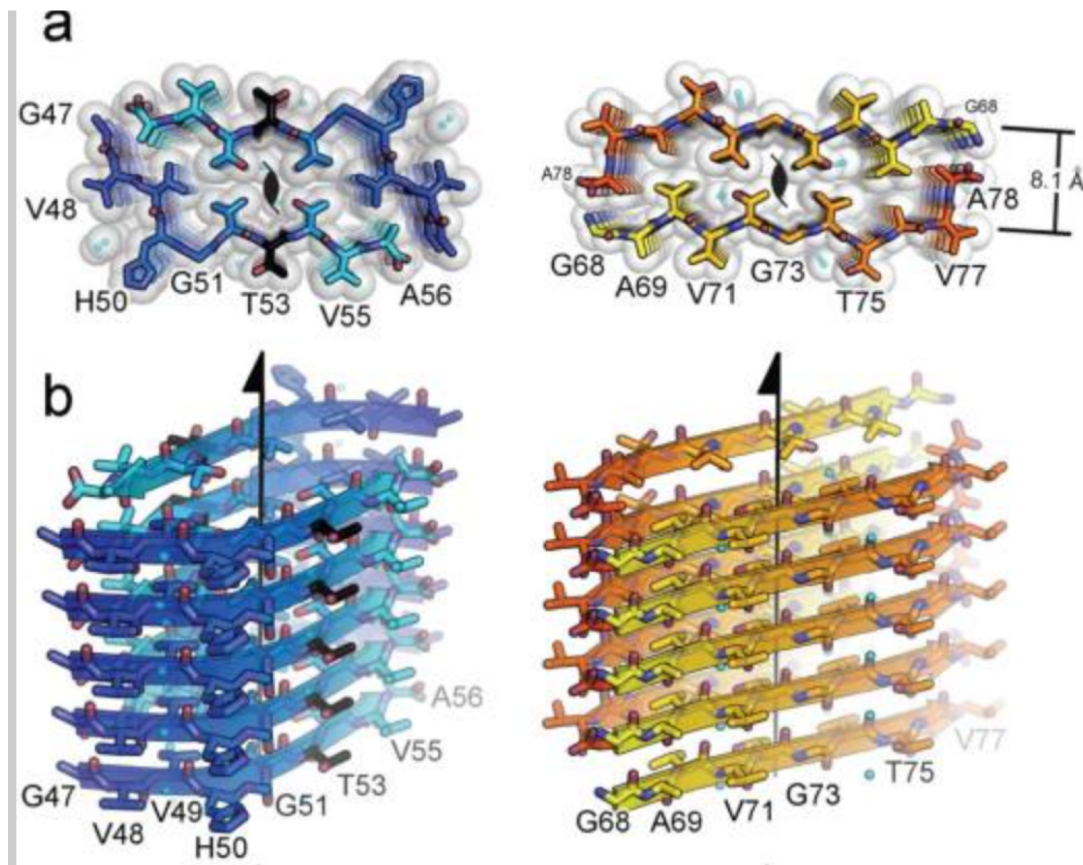


# Toxic core of $\alpha$ -synuclein from invisible crystals





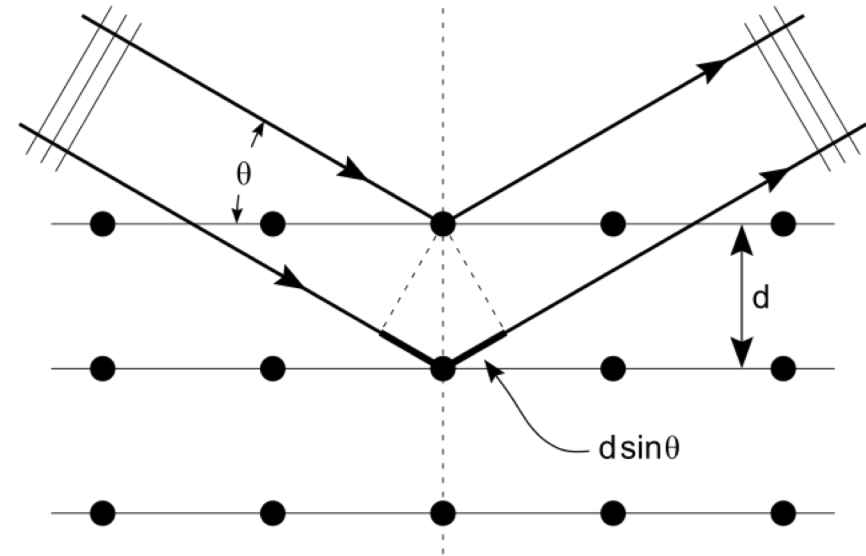
# Structure of Amyloid core



# Brief review of X-ray crystallography

# Diffraction Review

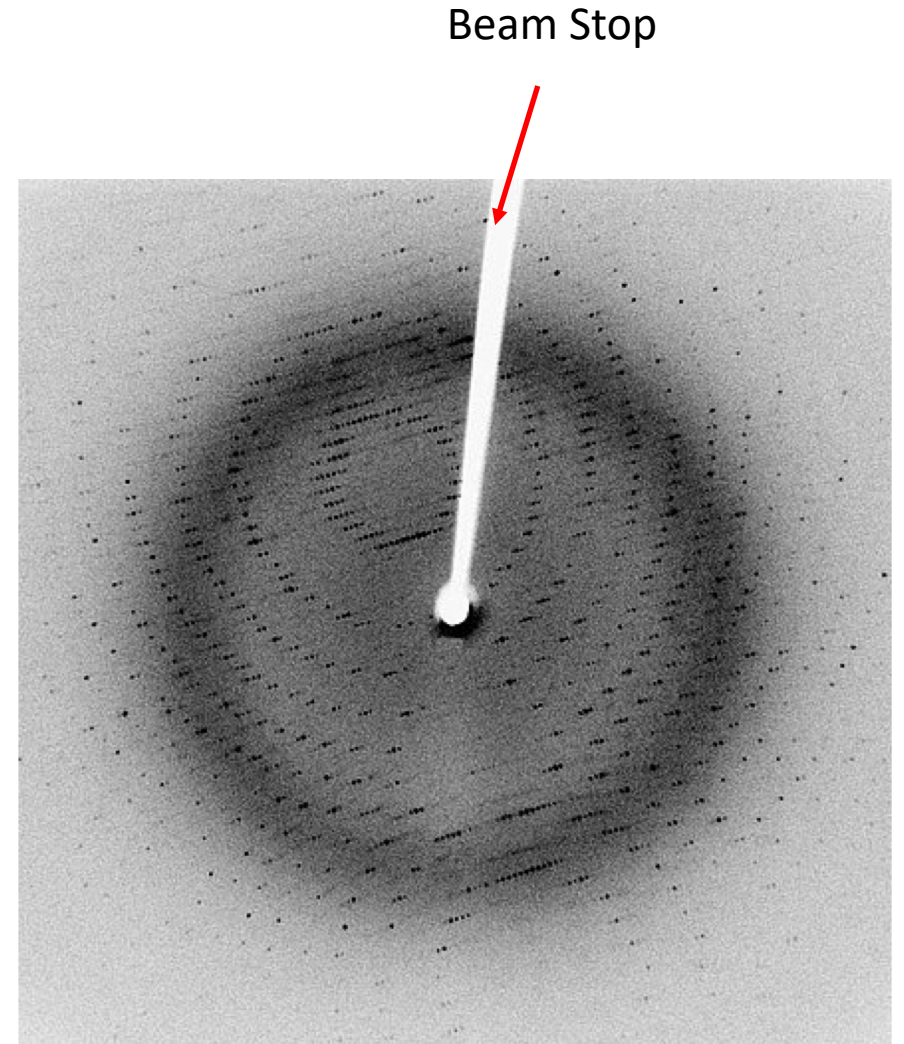
- Set of scattering points separated by distance  $d$
- Beam hits at angle  $\theta$  relative to plane
- Constructive interference only when their path length difference keeps them in phase
- Bragg's law
  - $n\lambda = 2d \sin \theta$





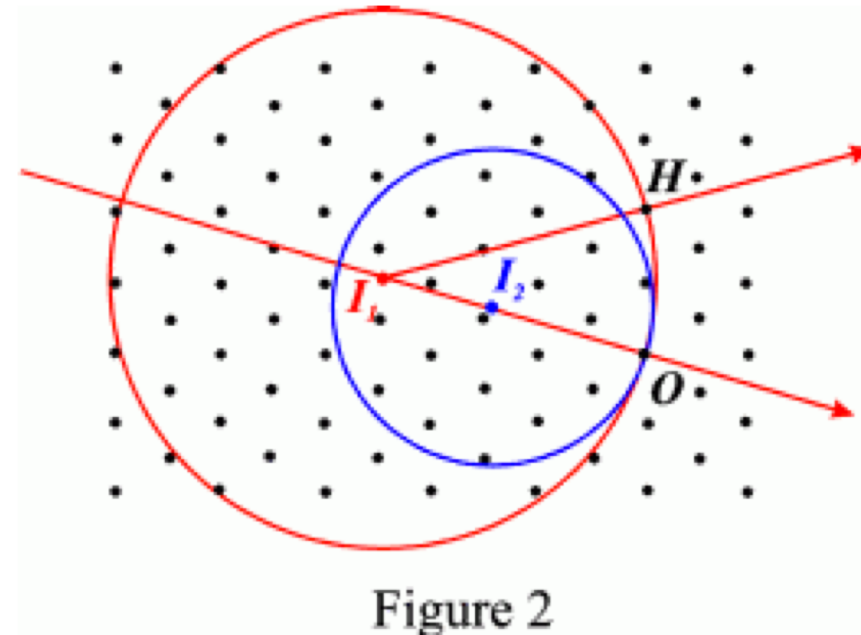
# X-Ray Diffraction

- Mount crystal, expose to x-ray beam at defined wavelength
- Collect images of reflections on detector
- Only collect intensities and positions, not phases
- Rotate crystal (180 deg) to get all reflections
- From positions, get 3D lattice parameters
- Phasing
  - Ab initio (small, high resolution)
  - Heavy atom derivatives
  - MAD/SAD
  - Molecular replacement



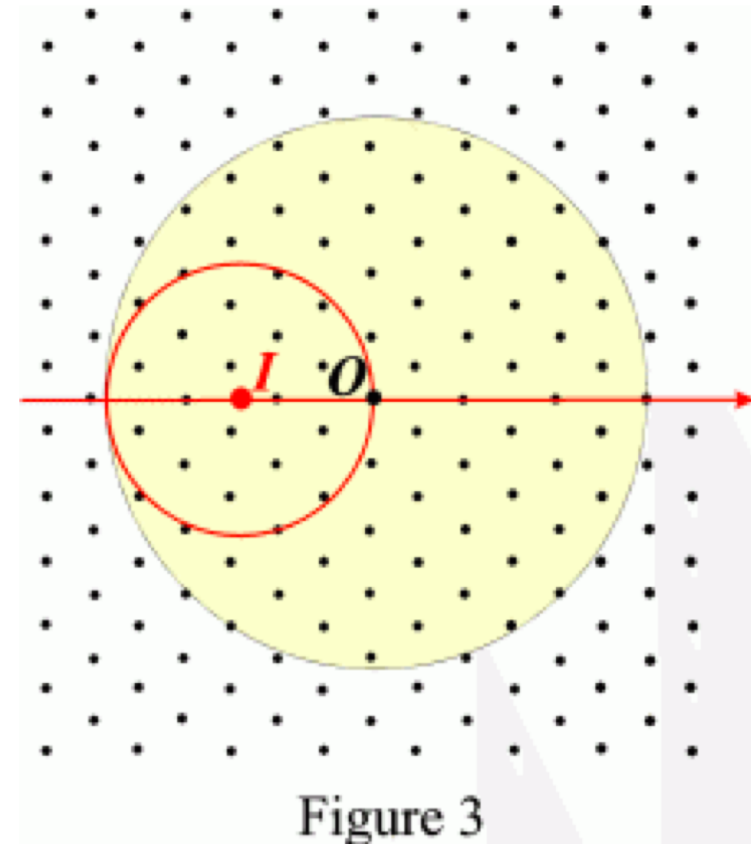
# Ewald Sphere

- Sphere of radius  $1/\lambda$  surrounding the crystal
- Only see diffraction spots which intersect the sphere
- For different wavelengths, get a differently sized sphere
- Rotate crystal on the beam to see different spots
- Xray:
  - $\lambda=0.709 \text{ \AA}$  (Ag Ka)
  - $\lambda=1.54 \text{ \AA}$  (Cu Ka)



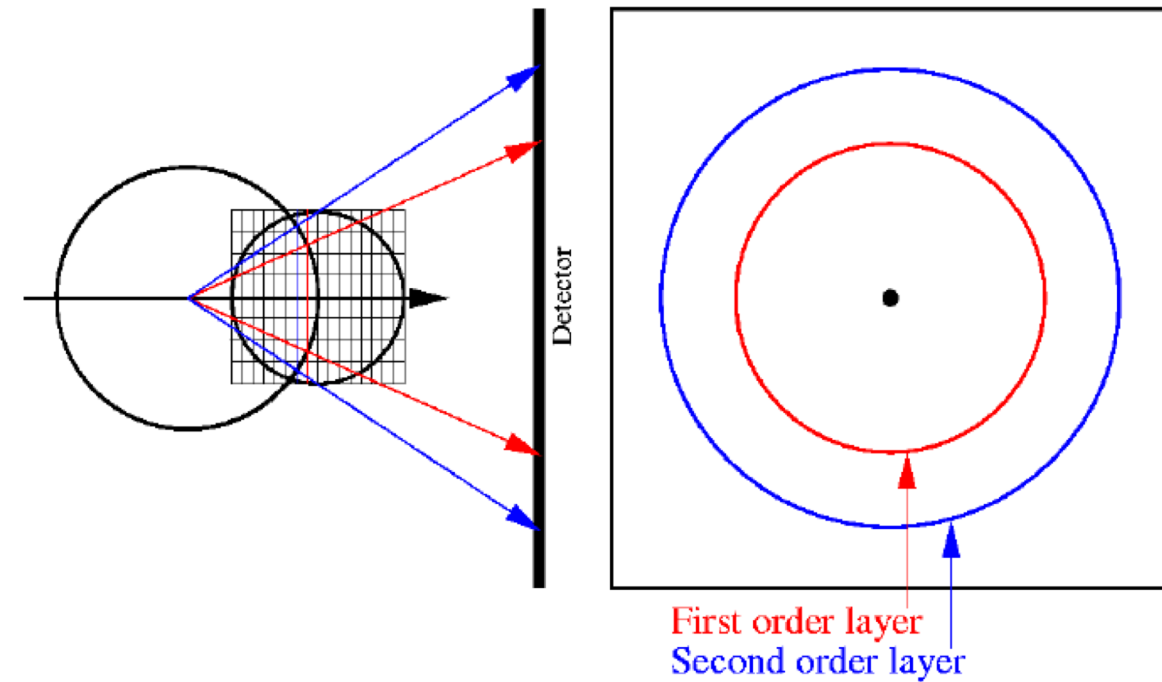
# Ewald Sphere

- If you rotate the crystal, the sphere rotates about the origin  $O$
- Yellow area is swept out
- Only observe reflections in the yellow area

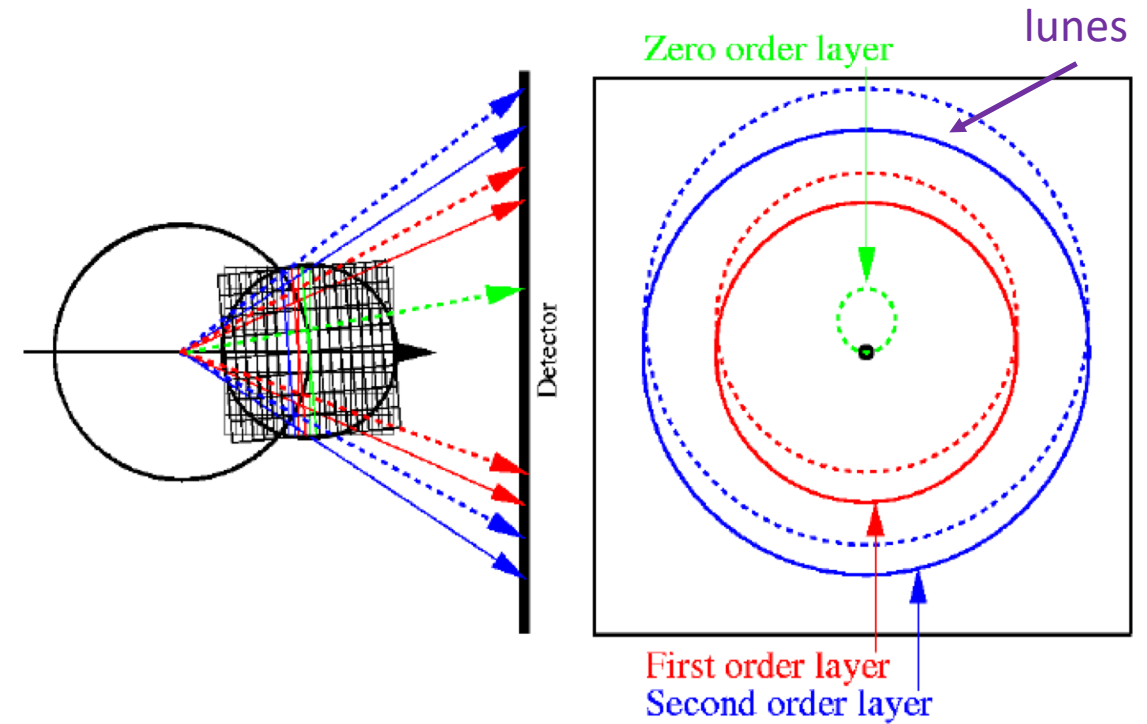


# Oscillation Method

## Still Image

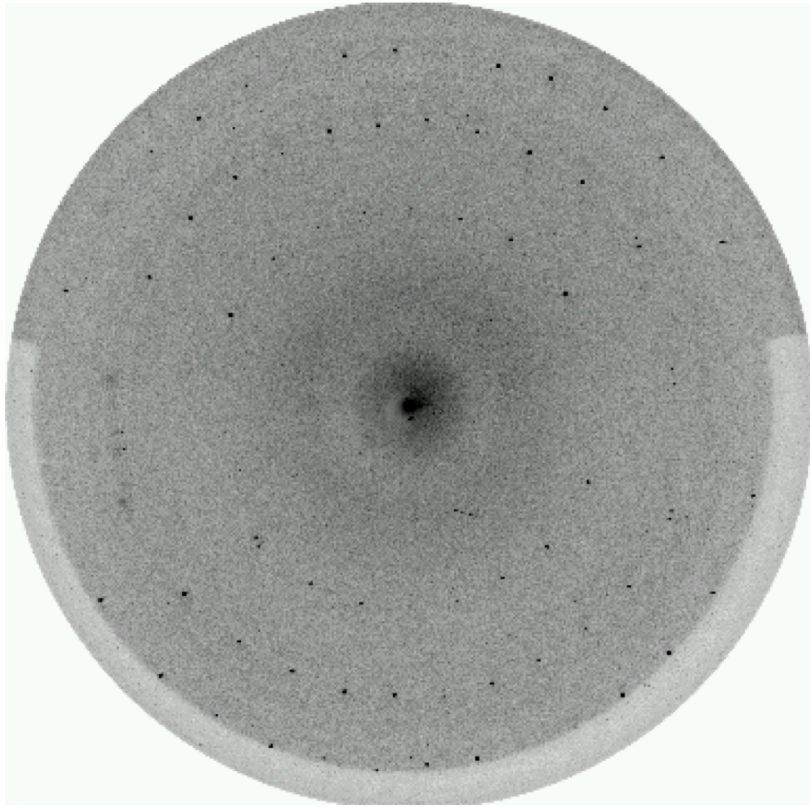


## Oscillating Image

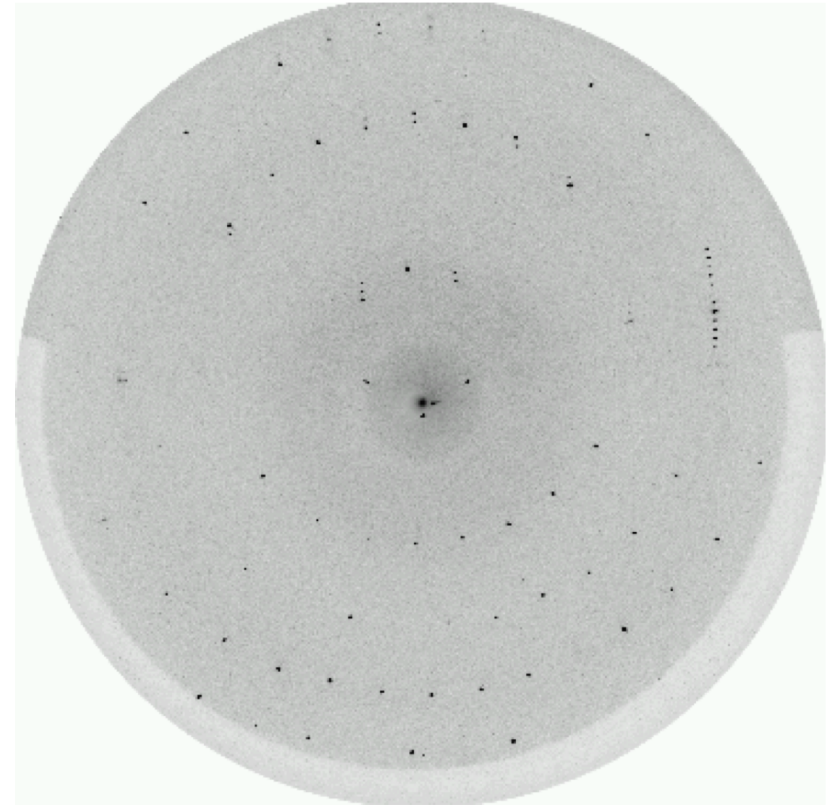


# Oscillation method

**Image 1**



**Rotate crystal 5 degrees, oscillate 0.5 degrees**





# Limitations of X-ray crystallography

- Approximately 30% of proteins that crystallize do not produce crystals large enough for x-ray diffraction experiments
  - Rupp, 2004; Quevillon-Cheruel et al., 2004
- XFEL?
  - Need many crystals
  - Expensive experiment

Back to EM

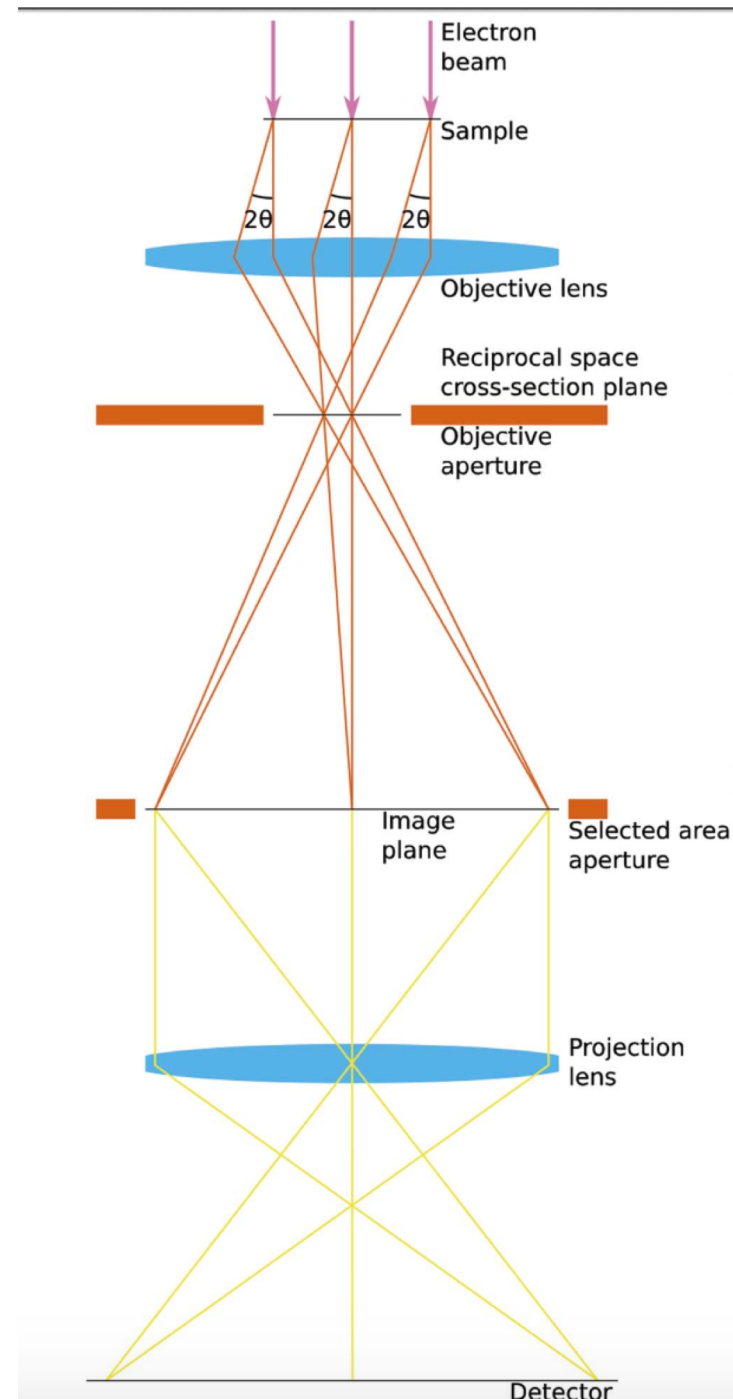
# Wavelengths

- X-ray
  - $\lambda=70.9$  pm (Ag Ka)
  - $\lambda =154$  pm (Cu Ka)
- EM
  - 80 keV: 4.18 pm
  - 120 keV: 3.35 pm
  - 200 keV: 2.51 pm
  - 300 keV: 1.97 pm

# Standard Optics

Objective aperture inserted

No SA aperture

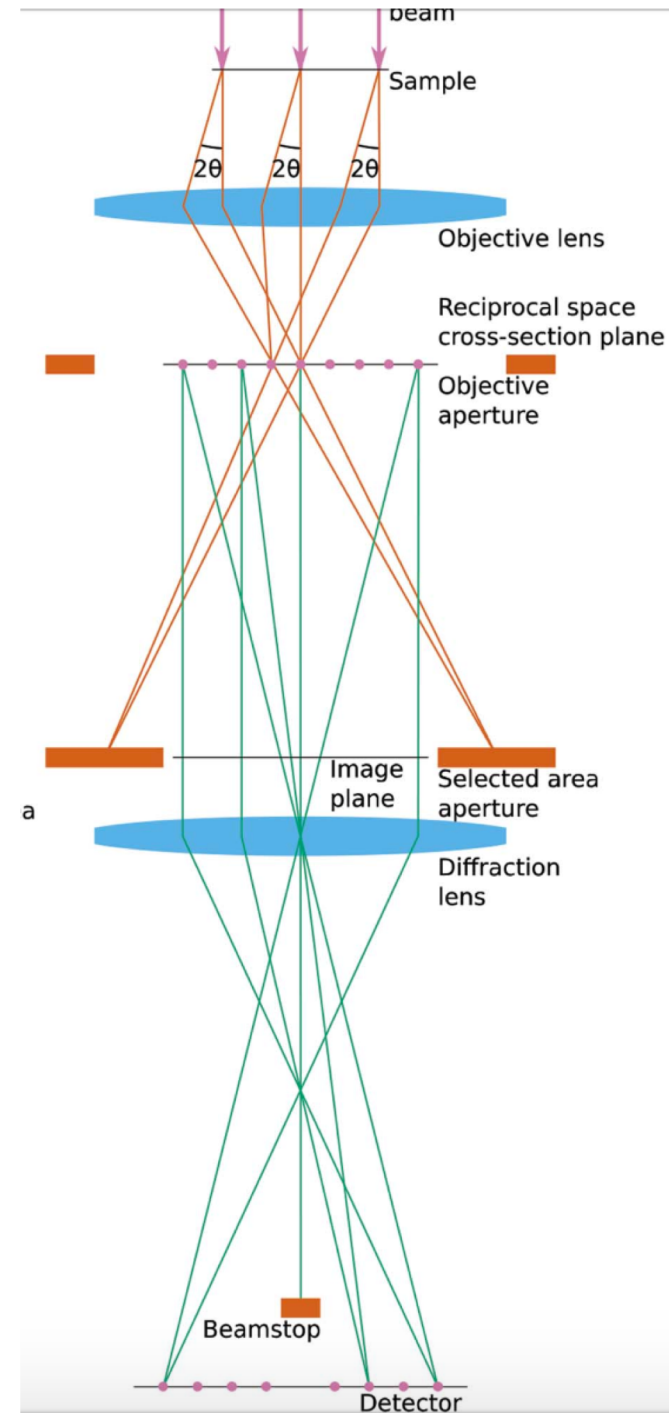


# Diffraction Optics

No objective aperture

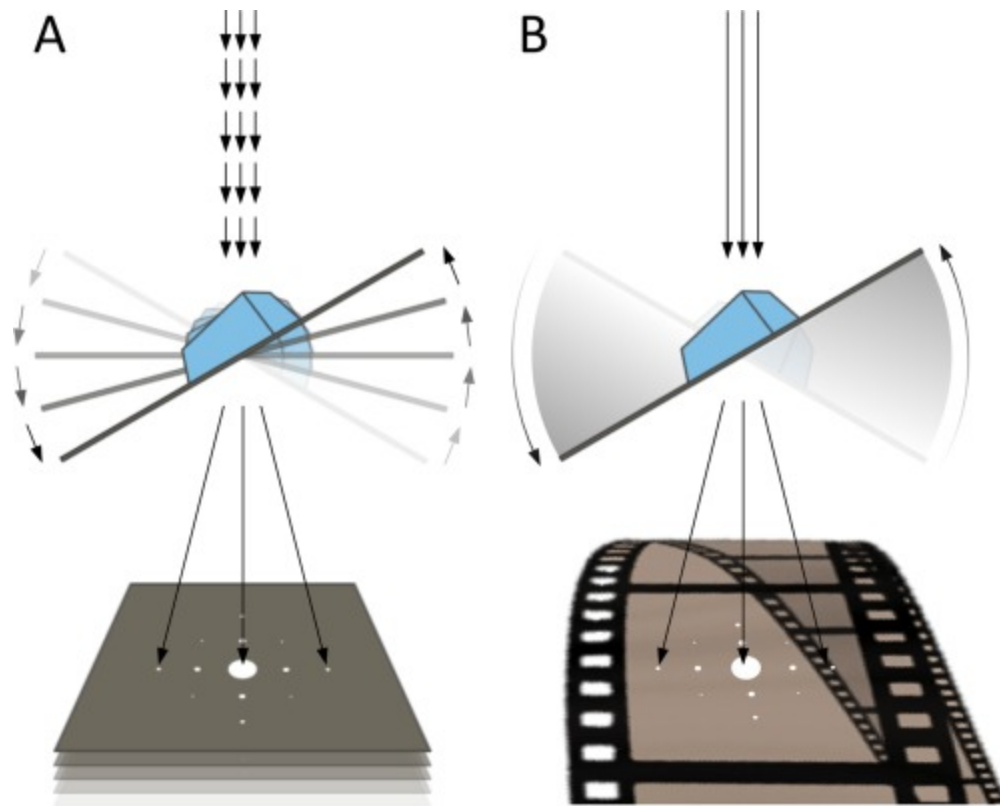
SA aperture inserted

Beamstop to block direct beam

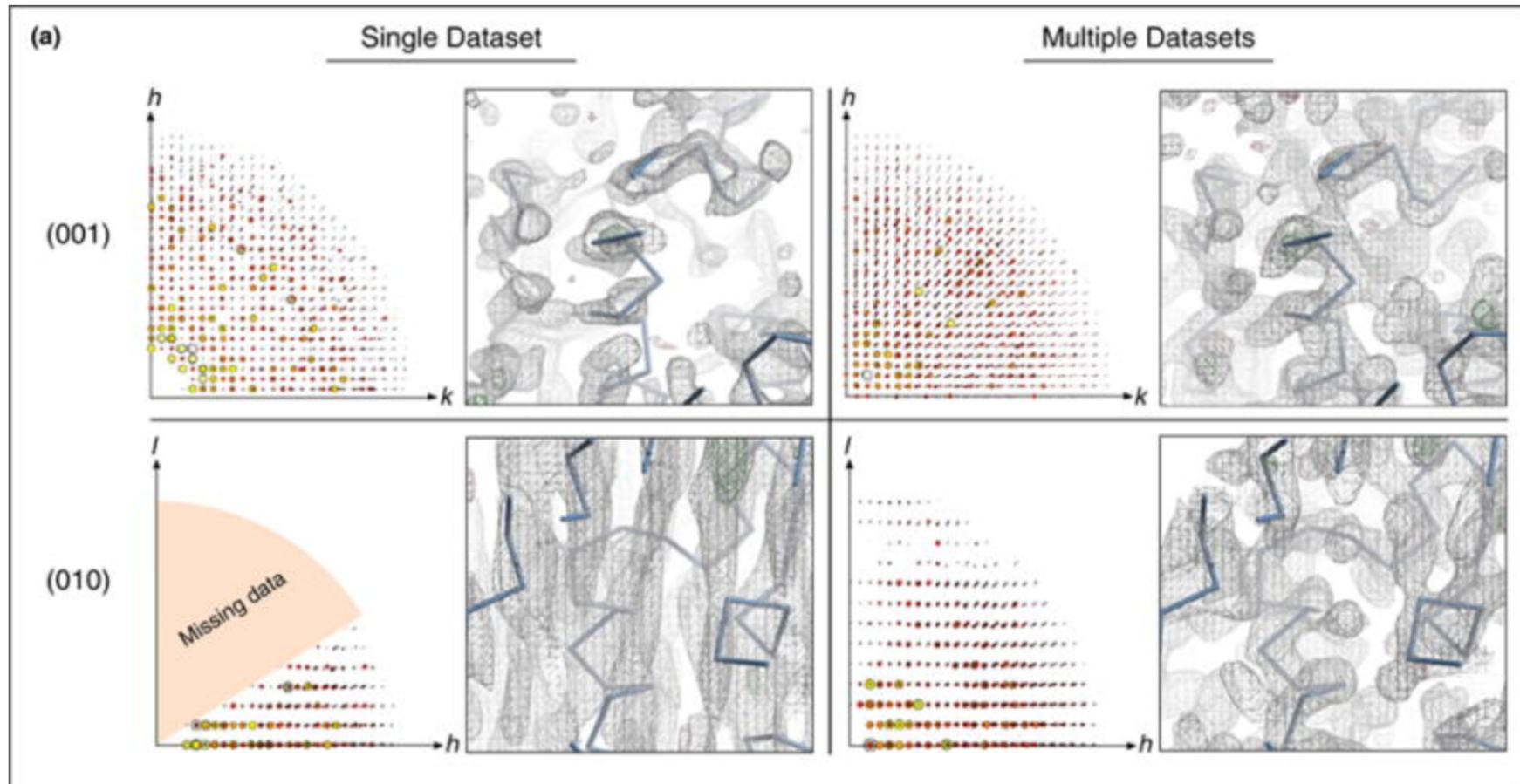




# Modes of Collection



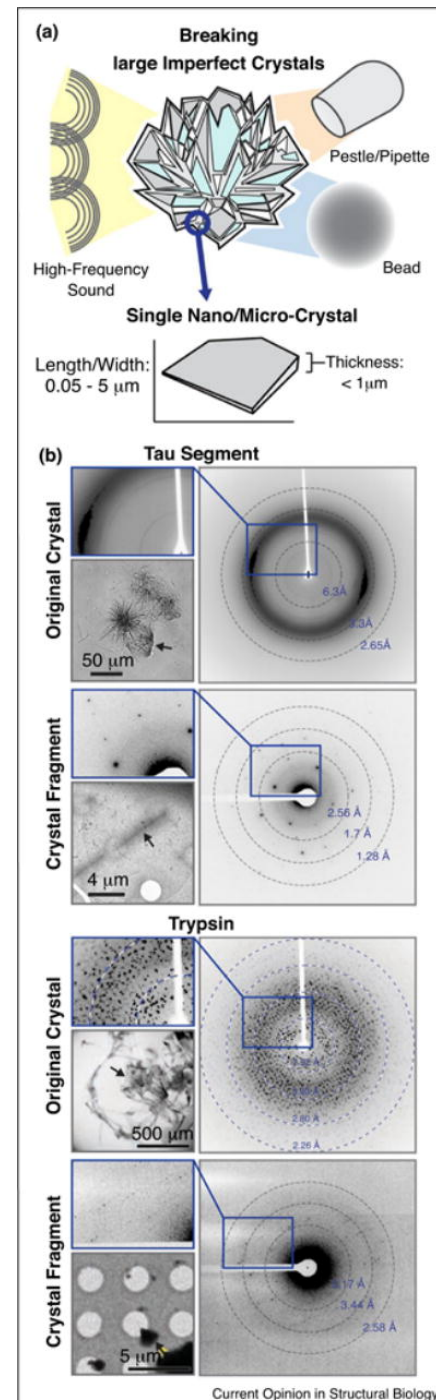
# Missing Wedge (-70 to +70 degrees)



# Crystal Thickness

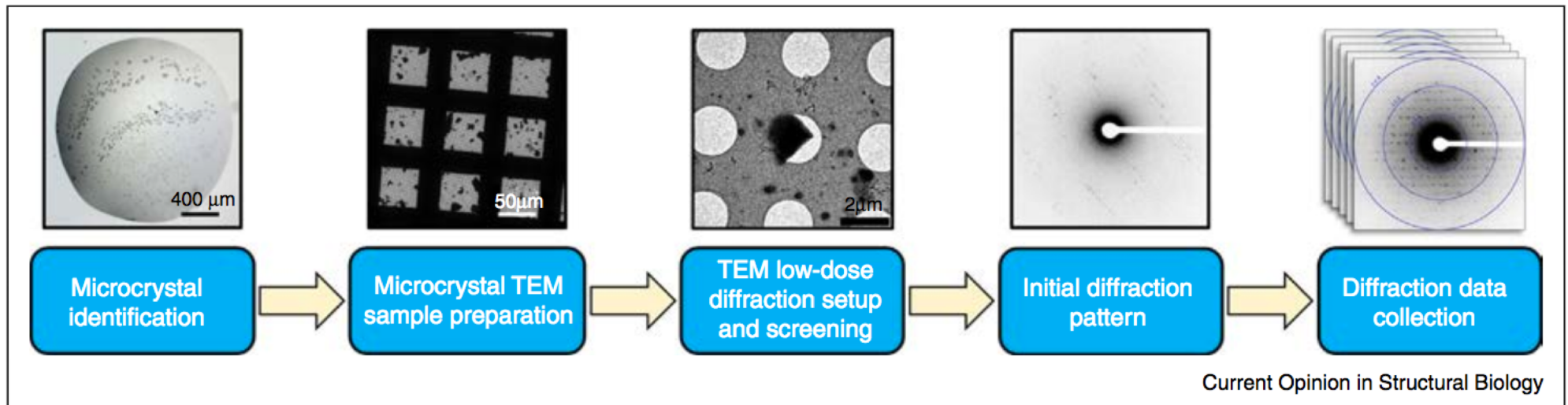
- Diffuse scattering: caused by partial disorder within crystal, as well as inelastic scattering
  - Increased background noise, errors in measurement of intensity levels
- Dynamic scattering: when inelastically scattered electrons have a second scattering effect
  - Intensities meant for a specific reflection are redistributed to other ones, leading to inaccuracies of integrated reflection counts
- Lysozyme: crystals thicker than 500 nm unusable
  - Maximum thickness may depend on packing and density

# Larger (imperfect) crystals



Details

# Workflow Overview



# Collection Setup: Initial screen

- Screen by negative stain for crystals
- Plunge freeze
  - Screen for optimal conditions to preserve crystals and have proper ice thickness
- Align microscope for low-dose electron diffraction
  - Optics well aligned for diffraction mode, diffraction astigmatism corrected
- Eucentric sample
- Screen at low mag (100X) for location of crystals and relative ice thickness
- Dose minimal:  $<10^{-6} \text{ e}^{-}\text{\AA}^2\text{s}^{-1}$

# Collection Setup: Crystal

- Examine crystals in over-focused diffraction mode
  - High contrast imaging at low dose:  $<10^{-3} \text{ e}^{-}\text{\AA}^2\text{s}^{-1}$
- Finely tune eucentricity at crystal location
- Set up diffraction: direct beam centered and blocked by beam stop
  - Dose rate  $0.01\text{-}0.05 \text{ e}^{-}\text{\AA}^2\text{s}^{-1}$
  - Beam  $5\text{-}10 \text{ }\mu\text{m}$  diameter
  - No objective aperture
  - Selected Area (SA) aperture inserted, approximately size of crystal
- Collect image: 2-5s
- If high quality diffraction seen: collect tilting data set



# Data Collection: Single Images

- Single images (like tomography)
- Discrete angles (0.5-1 degree increment)
- Can adjust exposure time depending on diffraction strength
- CMOS camera at best operating condition: enough time to re-charge electronics for each pixel, best signal to noise ratio
- BUT
- Due to Ewald sphere, most reflections are only partially recorded
- Need to either sum the partial observations or figure out what is the full intensity reflection
- Need special software for this processing

# Original implementation (Shi et al, 2013)

- Image single images at various tilts (1 deg increment)
  - Oscillation generally used in x-ray crystallography
- Reflections recorded in this manner are generally partial reflections
  - Needed in-house scripts to index the data and group symmetry-related reflections
- Lysozyme at 2.9 Å resolution
  - 200 keV on TVIPS F416 CMOS detector

# Three-dimensional electron crystallography of protein microcrystals.

Elife 2013 Nov 19

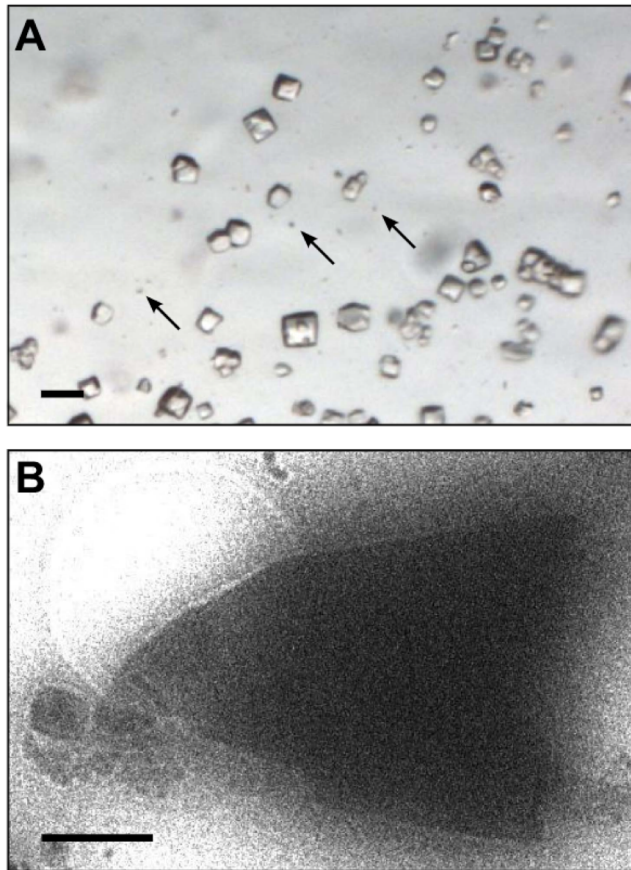


**Figure 1.** Images of lysozyme microcrystals. **(A)** Light micrograph showing lysozyme microcrystals (three examples indicated by arrows) in comparison with larger crystals of the size normally used for X-ray crystallography. Scale bar is 50  $\mu\text{m}$ . **(B)** Lysozyme microcrystals visualized in over-focused diffraction mode on the cryo-EM prior to data collection. The length and width of the crystals varied from 2 to 6  $\mu\text{m}$  with an estimated thickness of  $\sim 0.5\text{--}1\text{ }\mu\text{m}$ . Scale bar is 1  $\mu\text{m}$ .

DOI: [10.7554/eLife.01345.003](https://doi.org/10.7554/eLife.01345.003)

# Critical Dose for Diffraction Imaging

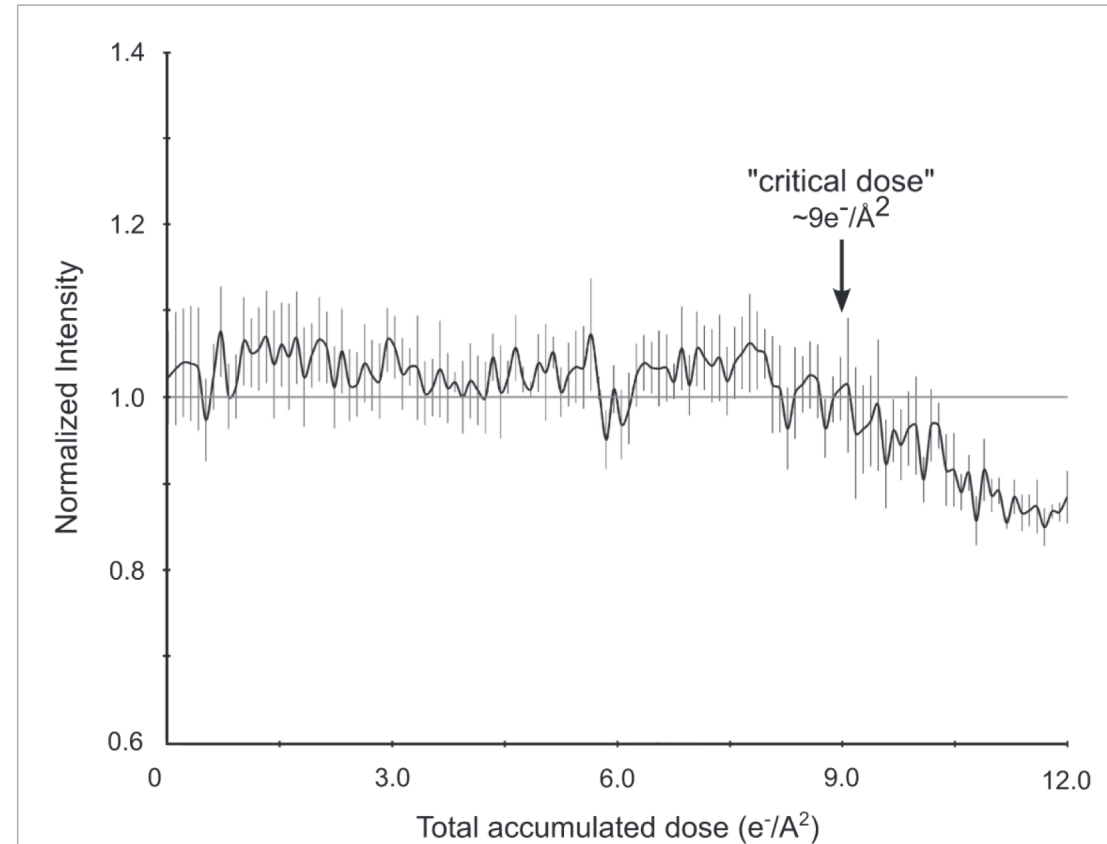


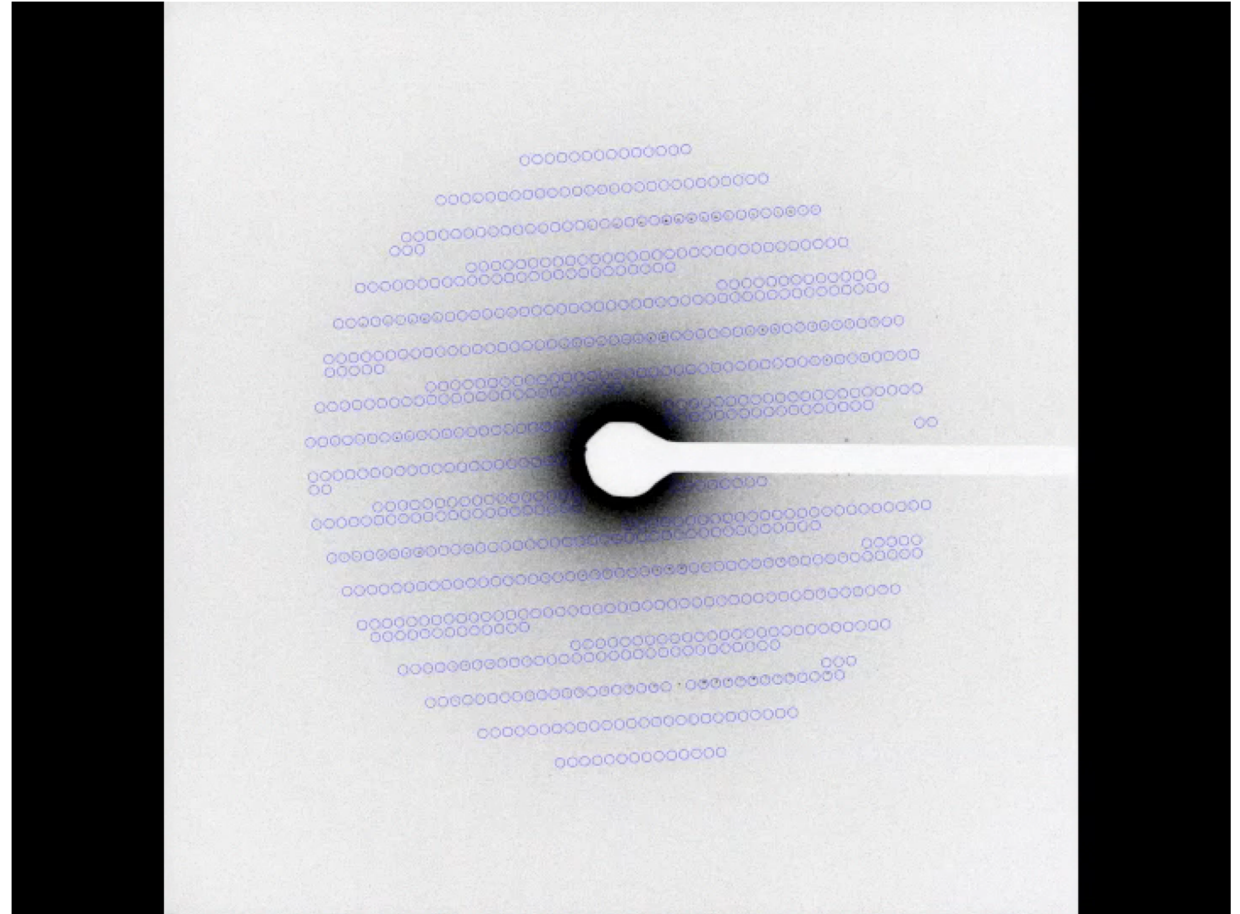
**Figure 3.** Effects of cumulative electron dose on diffraction data quality. A single lysozyme microcrystal was subjected to 120 sequential exposures without tilting, each of a dose of  $\sim 0.1 \text{ e}^-/\text{\AA}^2$  for a total accumulated dose of  $\sim 12 \text{ e}^-/\text{\AA}^2$ . Normalized intensity vs total accumulated dose for three diffraction spots observed over all 120 sequential frames was plotted. A decrease in diffraction intensity becomes apparent at a dosage of  $\sim 9 \text{ e}^-/\text{\AA}^2$  ('critical dose'). Bars represent standard error of the mean.

DOI: [10.7554/eLife.01345.005](https://doi.org/10.7554/eLife.01345.005)

# Diffraction from single crystal

**Video 1.** An example of a complete three-dimensional electron diffraction data set from a single lysozyme microcrystal. In this example, diffraction patterns were recorded at 1° intervals from a single crystal, tilted over 47°. Cumulative dose was  $\sim 5 \text{ e}^-/\text{\AA}^2$  in this example.

DOI: [10.7554/eLife.01345.006](https://doi.org/10.7554/eLife.01345.006)



# Small changes in tilt alter intensity

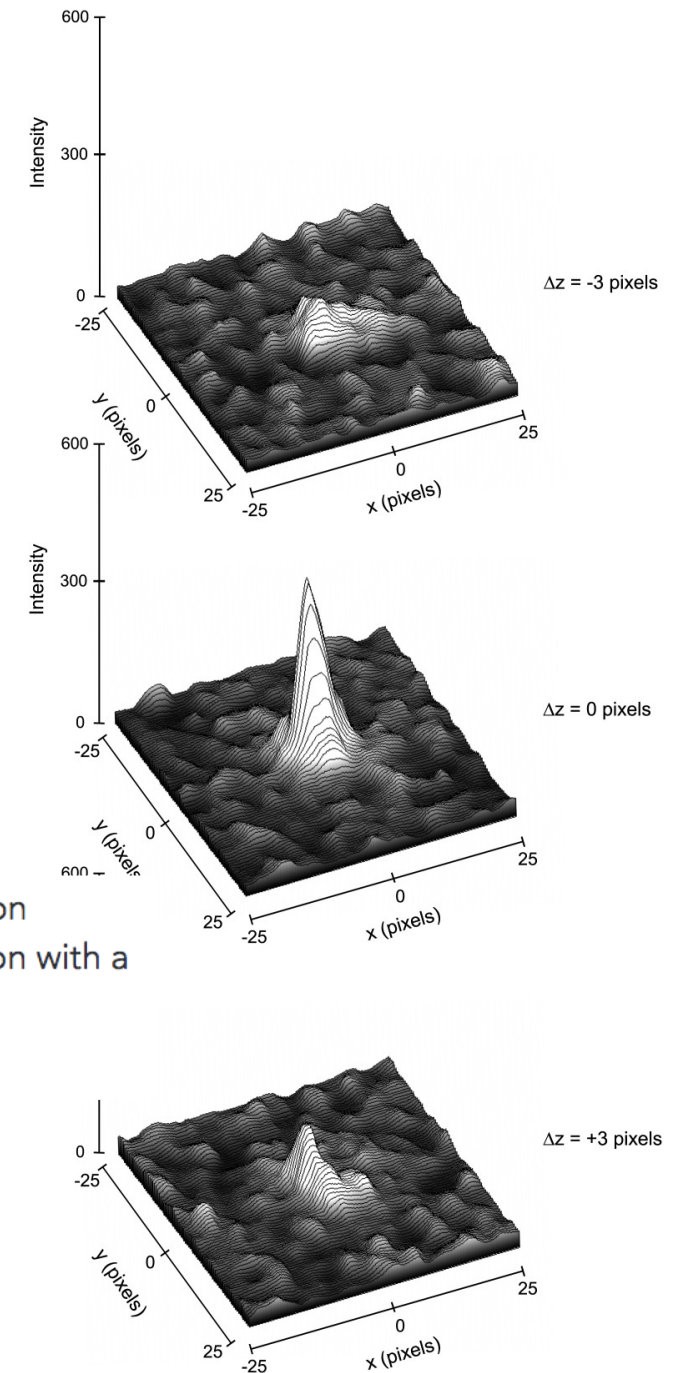


**Figure 5.** Three-dimensional profiles of the intensity of a single reflection over three consecutive diffraction patterns at  $-0.1^\circ$ ,  $0^\circ$ , and  $0.1^\circ$  degree tilts. The plots show the approximate dimensions of the full reflection with a width (full width at half maximum height) of 3–5 pixels in the x, y, and z direction.

DOI: [10.7554/eLife.01345.009](https://doi.org/10.7554/eLife.01345.009)

# Better Data Collection: Continuous rotation

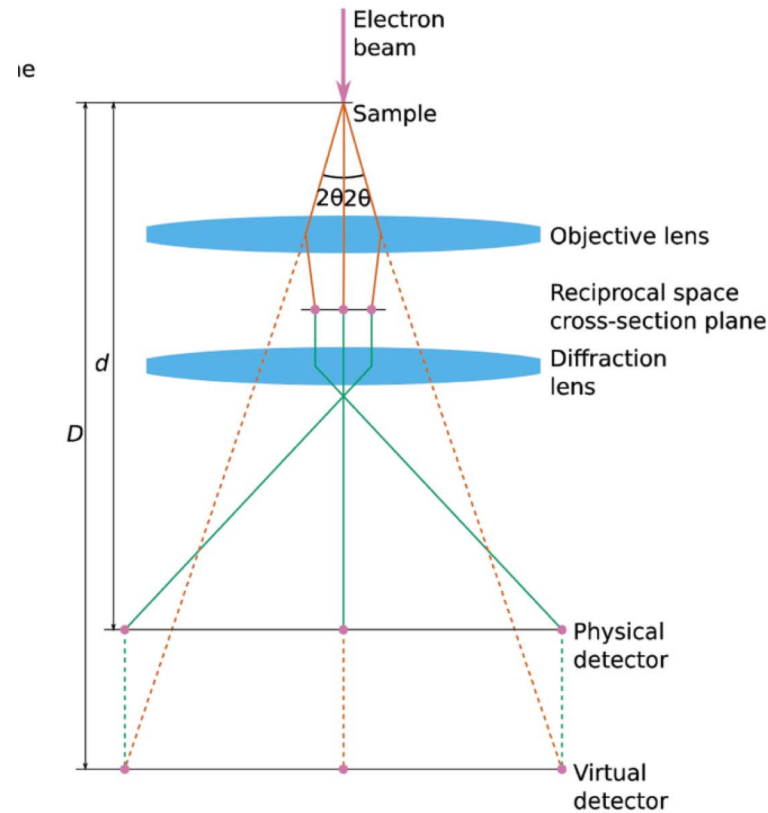
- Rotate stage at continuous rate
- Rotate to coordinate with exposure time
- Camera needs to be in continuous “rolling shutter” mode
- High rotation rate: increases the recorded reflection fraction on each frame
  - Too high: spot overlap
- Low rotation rate: makes weaker, high resolution reflections more visible
  - Too low: too few spots per image



# Data Collection: more specifics

- To date, most MicroED data was collected on a CMOS camera in “rolling shutter” mode
- Continuous readout of microscope parameters disabled
- In processing software, need to define
  - Beam Center
    - May not be center of image
    - May change due to microscope instabilities
  - Rotation rate of stage – angle and range of each frame
    - Need to record starting angle and direction (clockwise/counter-clockwise)
  - Virtual sample-detector distance
    - Calibrate from powder diffraction pattern of gold or graphite
- Conversion of movie to SMV (Super Marty View) format
  - Supported by x-ray software such as DIALS, MOSFLM, XDS

Lens magnification means physical distance to physical detector ( $d$ ) is smaller than distance to virtual detector ( $D$ )



# Processing Complications

- Interpretation of detector gain depends on downstream processing software
  - Ratio of variance and mean of intensities in background pixels
- Camera does not label hot or dead pixels
- Because patterns are collected at very low electron dose, even the strongest low-resolution reflections still within linear range
- Most standard software needs a configuration file for the camera and microscope: camera length, wavelength, tilt axis

# Indexing

- MOSFLM/AIMLESS and XDS
- Electron wavelength at 200 keV: 2.5 pm
  - Scattering angles small, Ewald sphere less curved
  - Each orientation is almost planar in reciprocal space
- 5-10 images spanning 20 degrees rotation wedge are generally enough for autoindexing
- Sample orientation calculated from the rotation rate and image timestamp
  - Large inaccuracies in initial estimate of rotation angle
- Errors in crystal orientation: absorb residual errors in the mosaicity
  - Mosaicity then acts as a sink for errors, not a model of lattice disorder

# Phasing

- For most structures, phasing was done through molecular replacement
- Standard X-ray crystallography tools
- CNS, Phaser, phenix.refine, REFMAC all have electron scattering factors built in
- Ab initio phasing: has been done for small peptides
  - Need diffraction to 1.4 Å or better

# Extended Data Table: Same as for x-ray crystallography

Extended Data Table 1

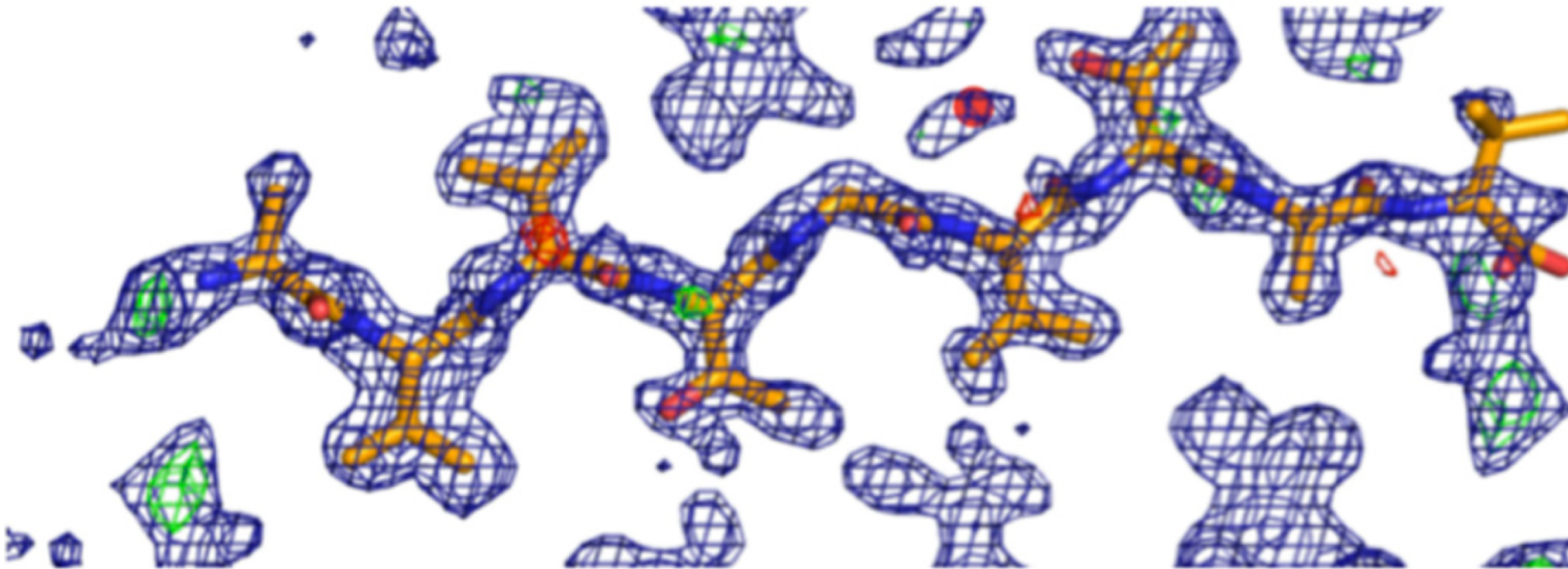
Statistics of data collection and atomic refinement for NACore, its fragment SubNACore, and PreNAC.

Segment	SubNACore AVVTGVTAV	NACore GAVVTGVTAVA	PreNAC GVVHGVTTVA
Data collection			
Radiation source	Synchrotron	Electron	Electron
Space group	C2	C2	P21
Cell dimensions			
<i>a,b,c</i> (Å)	61.9, 4.80, 17.3	70.8, 4.82, 16.79	17.9, 4.7, 33.0
$\alpha,\beta,\gamma$ (°)	90, 104.1, 90	90, 105.7, 90	90, 94.3, 90
Resolution (Å)	1.85 (1.95–1.85)	1.43 (1.60–1.43)	1.41 (1.56–1.41)
Wavelength (Å)	0.9791	0.0251	0.0251
<i>R</i> <sub>merge</sub>	0.117 (0.282)	0.173 (0.560)	0.236 (0.535)
<i>R</i> <sub>r.i.m.</sub>	0.135 (0.322)	0.199 (0.647)	0.264 (0.609)
<i>R</i> <sub>p.i.m.</sub>	0.065 (0.154)	0.093 (0.311)	0.185 (0.305)
<i>I</i> / $\sigma$ <i>I</i>	5.2 (2.7)	5.5 (2.5)	4.6 (1.8)
CC <sub>1/2</sub> (%)	99.5 (97.8)	99.4 (92.3)	96.7(74.0)
Completeness (%)	97.9 (98.3)	89.9 (82.6)	86.9 (69.6)
Multiplicity	4.1 (4.0)	4.4 (4.3)	3.7 (3.5)
Refinement			
Resolution (Å)	1.85 (2.07–1.85)	1.43 (1.60–1.43)	1.41 (1.41–1.57)
No. reflections	470 (125)	1073 (245)	1006 (239)

\* Highest resolution shell is shown in parenthesis.

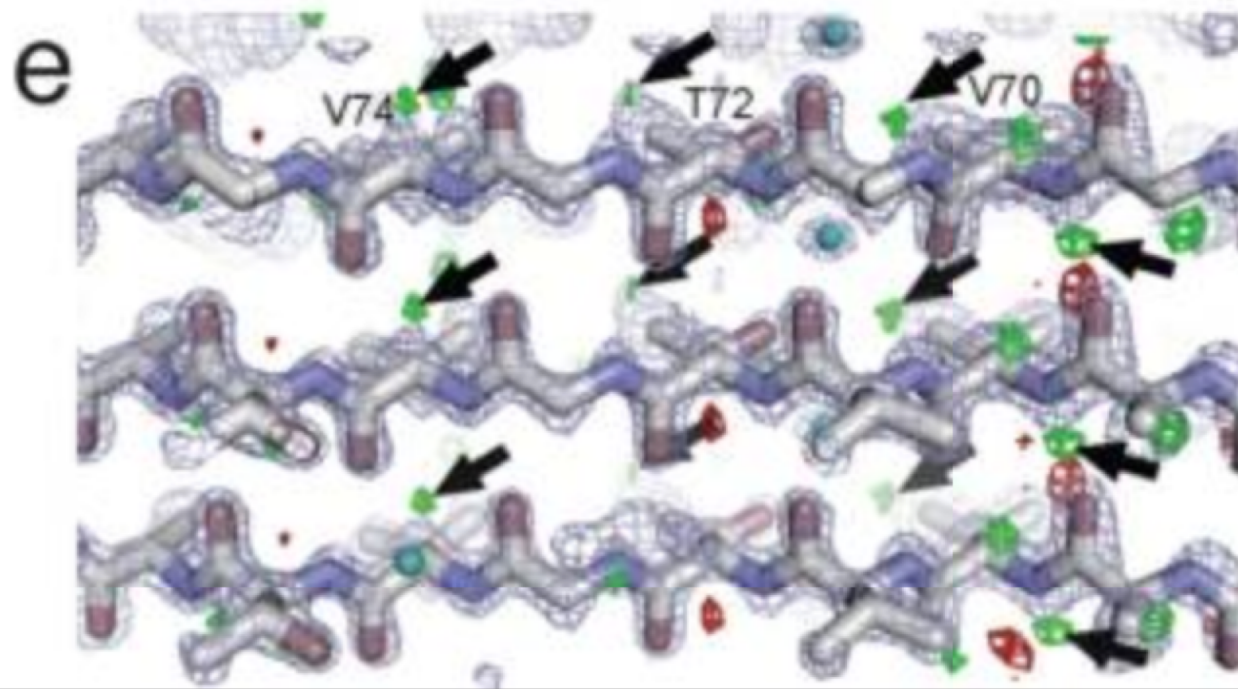


# Structure of Amyloid core



Difference density maps calculated after successful molecular replacement using the SubNACore search model clearly revealed the positions of the missing residues (positive  $F_o-F_c$  density at N and C termini corresponding to G68 and A78) and one water molecule near a threonine side chain (red circle); a second water was located during the refinement process. The blue mesh represents  $2F_o-F_c$  density contoured at 1.2  $\sigma$  level. The green and red mesh represent  $F_o-F_c$  density contoured at 3.0 and  $-3.0$   $\sigma$ , respectively. All maps were  $\sigma_a$ -weighted<sup>61</sup>.

2Fo-Fc Density map shows location of 5/73 protons (green)



# Thick Crystals

All rights reserved. No reuse allowed without permission.

## Collection of continuous rotation MicroED Data from Ion Beam Milled Crystals of Any Size

Michael W. Martynowycz,<sup>1,2</sup> Wei Zhao,<sup>3</sup> Johan Hattne,<sup>1,2</sup> Grant J. Jensen,<sup>3,4</sup> and Tamir Gonen,<sup>1,2,5,\*</sup>

<sup>1</sup> Howard Hughes Medical Institute, University of California, Los Angeles, Los Angeles, CA

<sup>2</sup> Department of Biological Chemistry, University of California, Los Angeles, Los Angeles, CA

<sup>3</sup> Department of Biology and Biological Engineering, California Institute of Technology, Pasadena, CA

<sup>4</sup> Howard Hughes Medical Institute, California Institute of Technology, Pasadena, CA

<sup>5</sup> Department of Physiology, University of California, Los Angeles, Los Angeles, CA

\* To whom correspondence should be sent: [tgonen@ucla.edu](mailto:tgonen@ucla.edu)

J Struct Biol. 2019 Mar 1;205(3):59-64. doi: 10.1016/j.jsb.2019.02.004. Epub 2019 Feb 20.

### Using focus ion beam to prepare crystal lamella for electron diffraction.

Zhou H<sup>1</sup>, Luo Z<sup>1</sup>, Li X<sup>2</sup>.

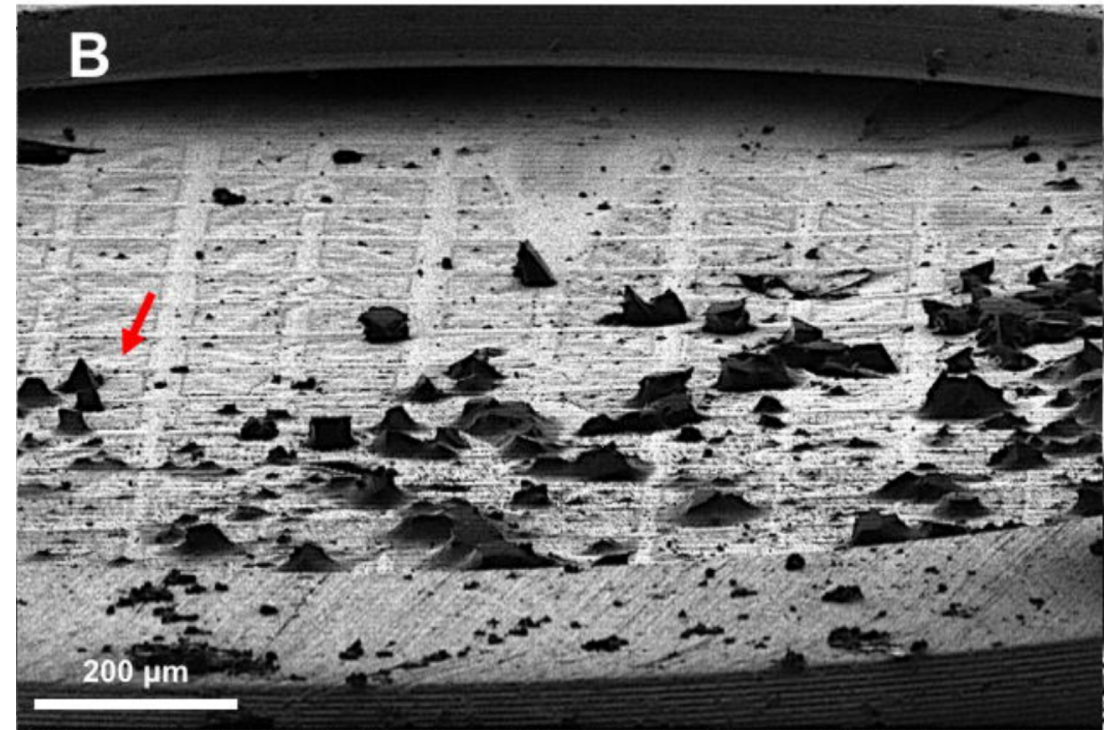
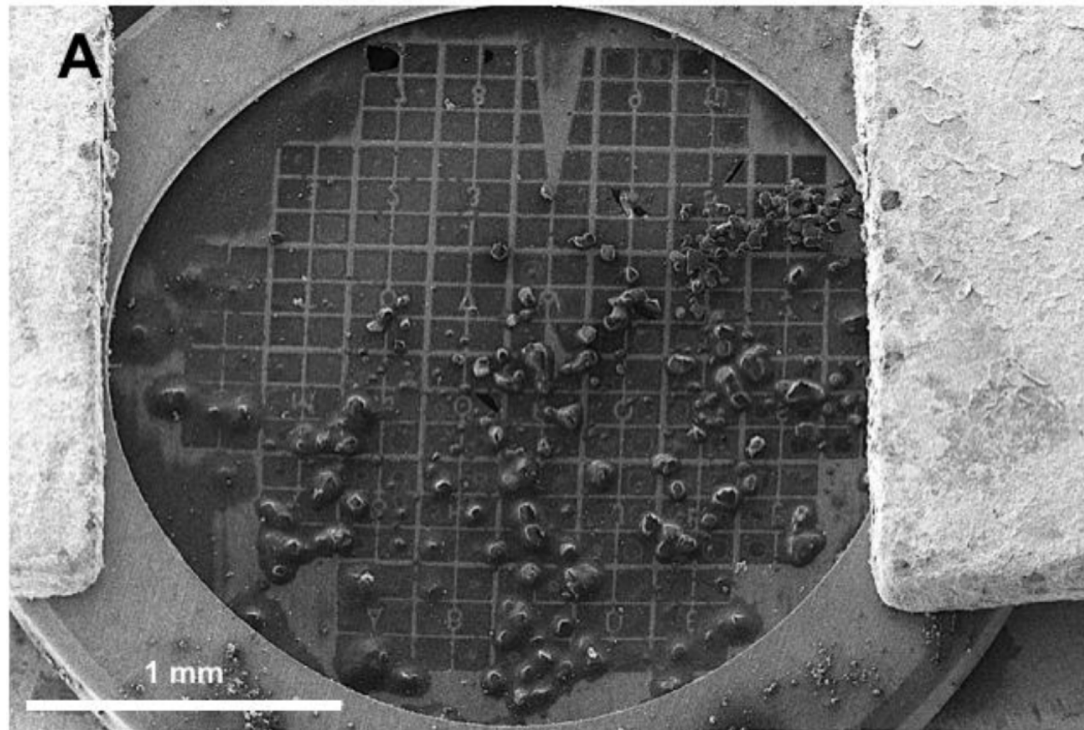
 Author information

#### Abstract

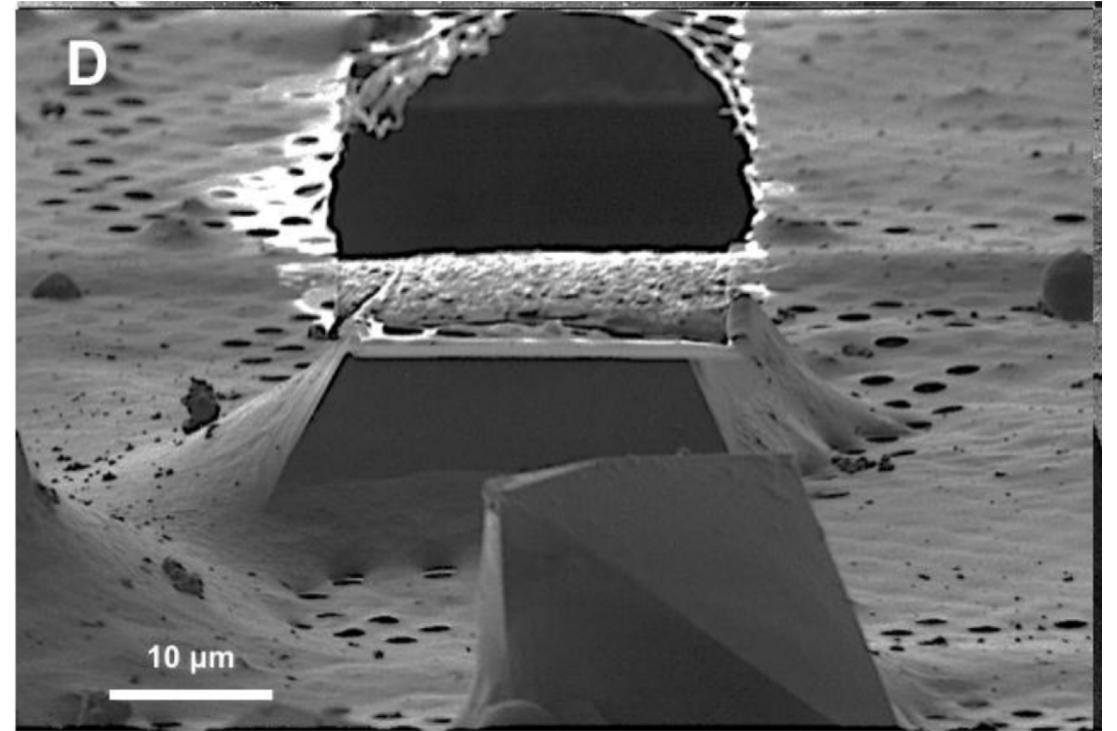
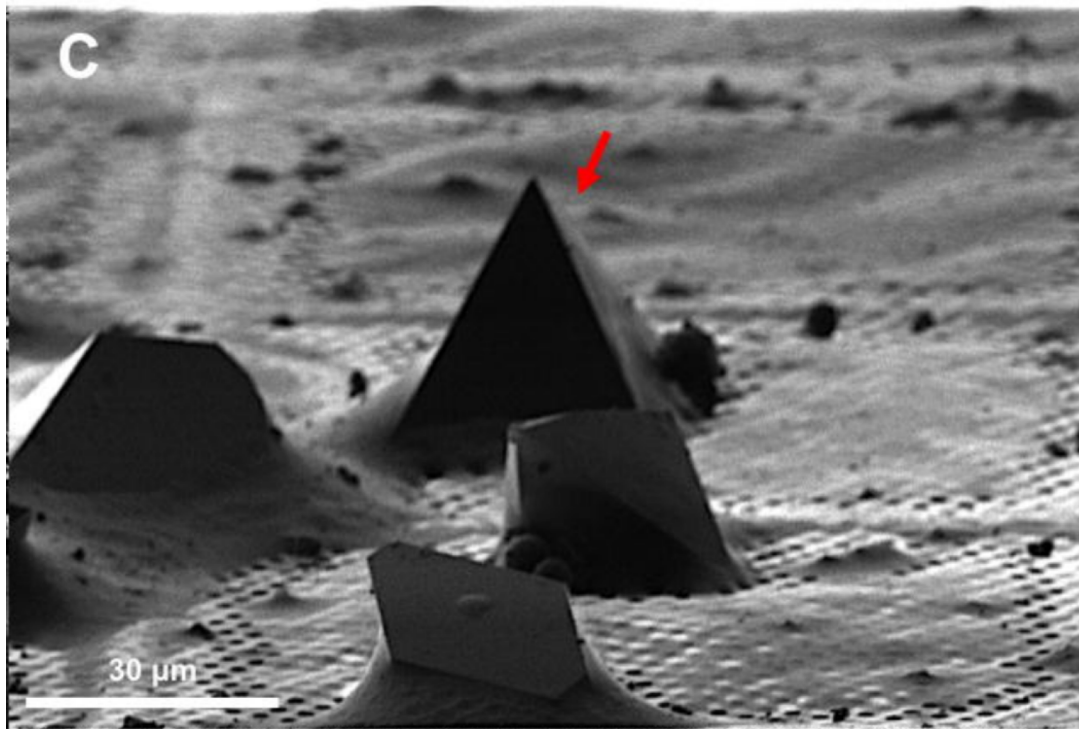
Electron diffraction provides a powerful tool to solve the structures of small protein crystals. However, strong interactions between the electrons and the materials limit the application of the electron crystallographic method on large protein crystals with micrometer or larger sizes. Here, we used the focused ion beam (FIB) equipped on the scanning electron microscope (SEM) to mill a large crystal to thin lamella. The influences of the milling on the crystal lamella were observed and investigated, including radiation damage on the crystal surface during the FIB imaging, deformation of the thin crystal lamella, and variation in the diffraction intensities under electron radiation. These observations provide important information to optimize the FIB milling, and hence is important to obtain high-quality crystal samples for routine structure determination of protein crystals using the electron cryo-microscope.



Use a FIB to thin them



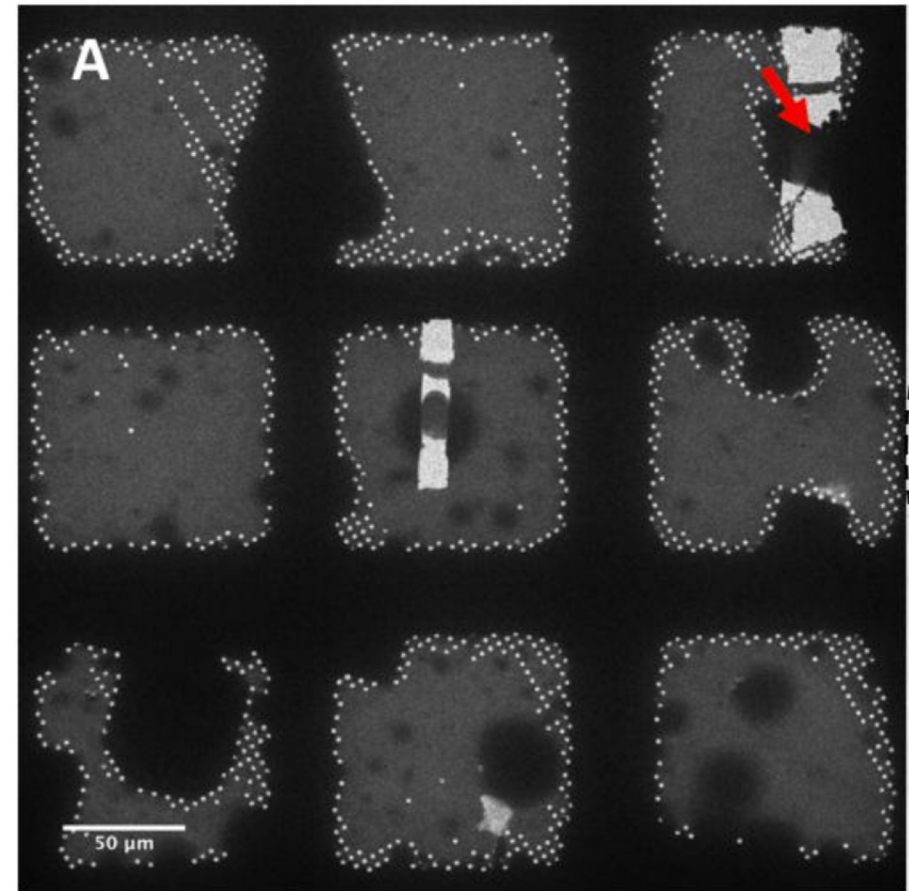
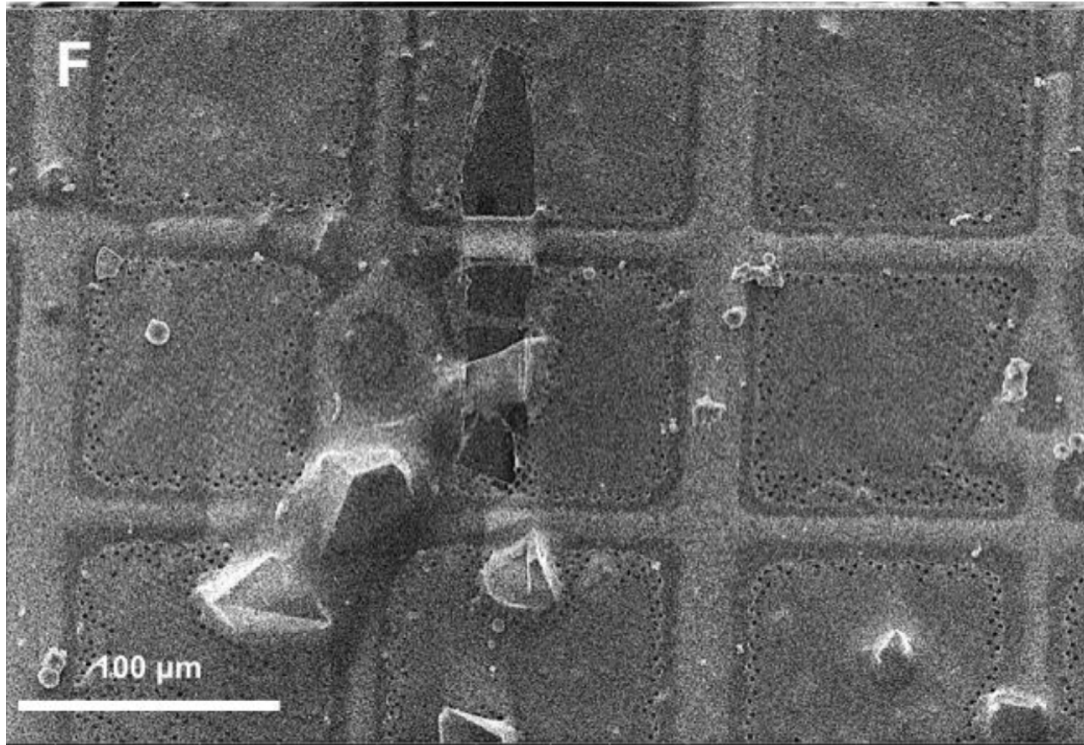
# Ion beam view, before and after



Thin to 300 nm

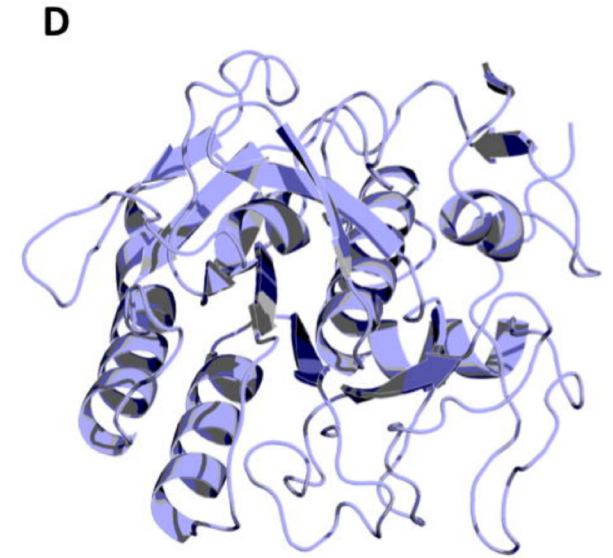
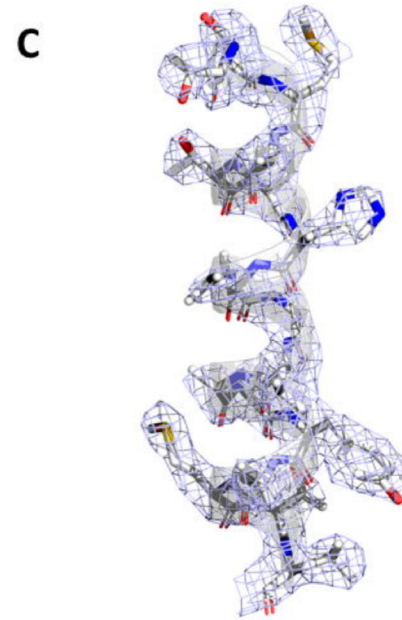
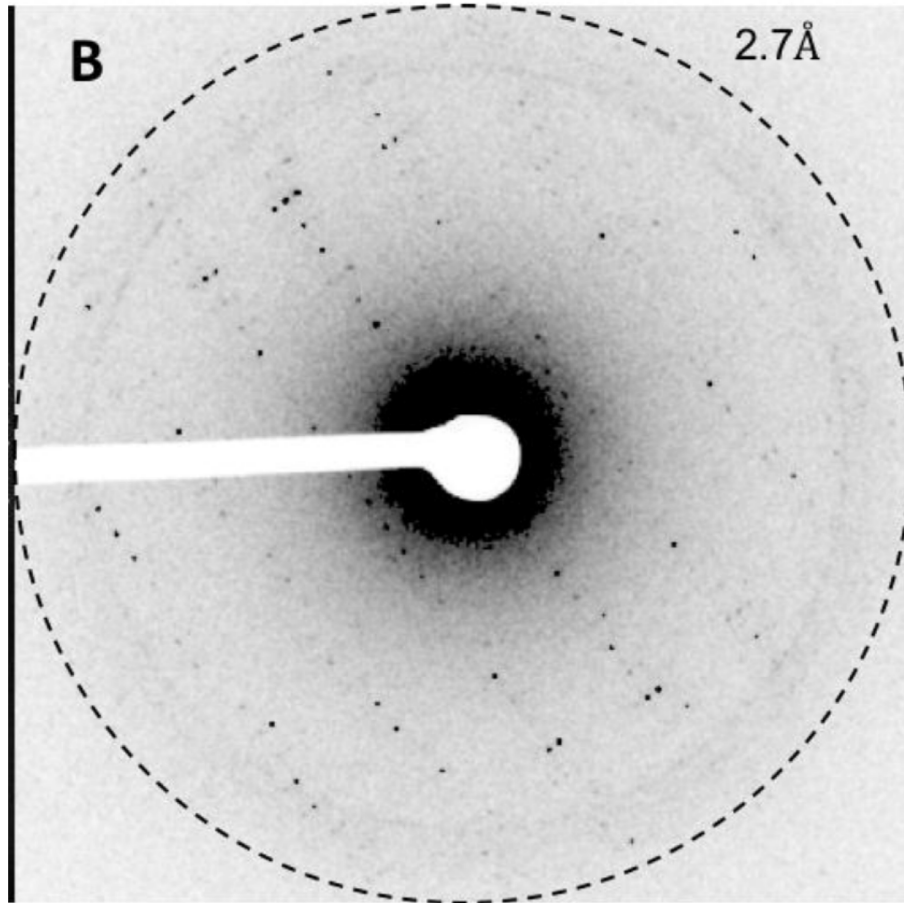


# Ebeam: SEM and TEM





# Proteinease K at 2.7 Å Resolution



# 2018: Breakthrough for organic molecules

- Realized that quickly solving structures of small organic molecules (drugs and drug candidates) is highly desired
- Purified powders can be placed directly on an EM grid
  - Dry, not in solution
- Possible to image even at RT
- Possible to put multiple samples on one grid
- Each crystal collection is relatively fast
- Molecules small enough to solve by direct phasing methods

# Small Molecules



Research Article

Cite This: *ACS Cent. Sci.* 2018, 4, 1587–1592


<http://pubs.acs.org/journal/acscii>

## The CryoEM Method MicroED as a Powerful Tool for Small Molecule Structure Determination

Christopher G. Jones,<sup>†,‡</sup> Michael W. Martynowycz,<sup>‡,‡</sup> Johan Hattne,<sup>‡</sup> Tyler J. Fulton,<sup>§</sup>  
Brian M. Stoltz,<sup>\*,§</sup> Jose A. Rodriguez,<sup>\*,†,||</sup> Hosea M. Nelson,<sup>\*,†</sup> and Tamir Gonen<sup>\*,‡</sup>

<sup>†</sup>Department of Chemistry and Biochemistry, <sup>‡</sup>Howard Hughes Medical Institute, David Geffen School of Medicine, Departments of Biological Chemistry and Physiology, and <sup>||</sup>UCLA-DOE Institute, University of California, Los Angeles, California 90095, United States

<sup>§</sup>The Warren and Katharine Schlinger Laboratory of Chemistry and Chemical Engineering, California Institute of Technology, Pasadena, California 91125, United States

 Supporting Information

# Small Molecules

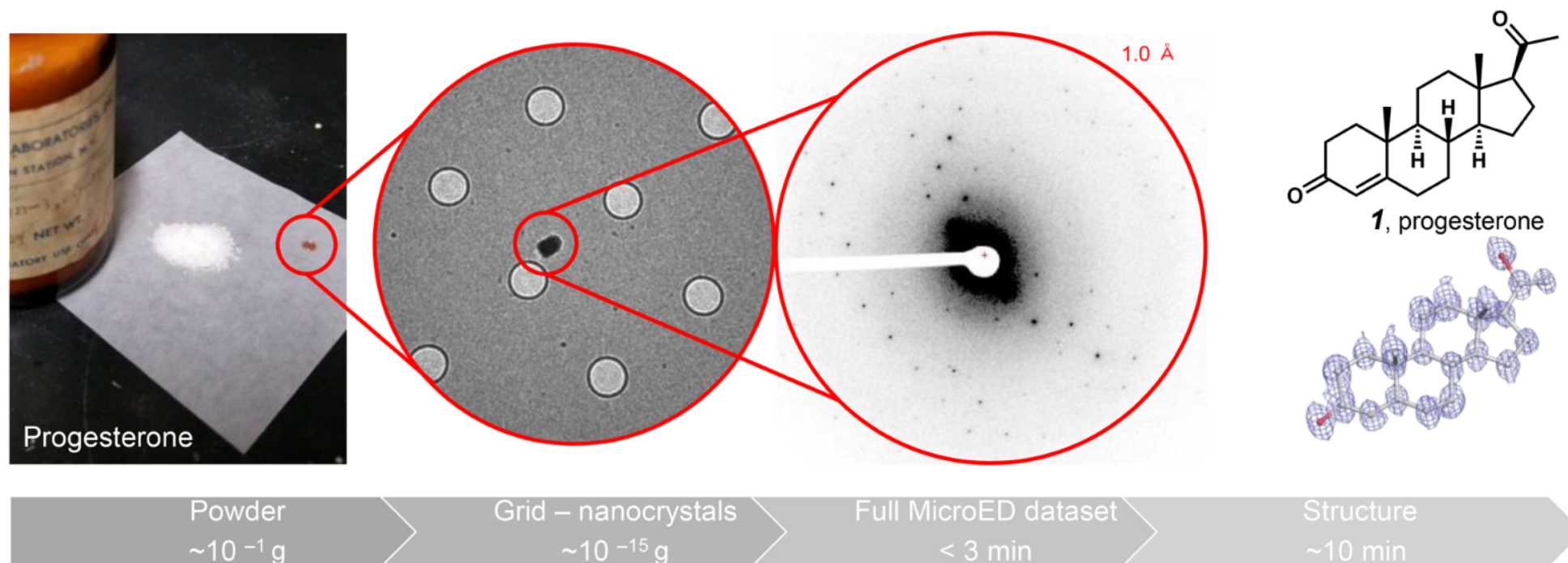
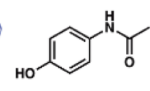
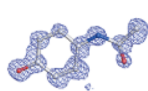


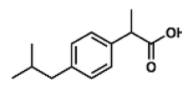
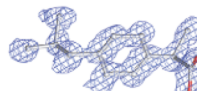
**Figure 1.** Process of applying MicroED to small molecule structural analysis. Here commercial progesterone (1) was analyzed, and an atomic resolution structure was determined at  $1 \text{ \AA}$  resolution. Grid holes are  $1 \mu\text{m}$  in diameter.

# Small Molecules

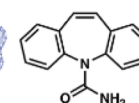
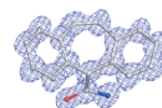
**A**



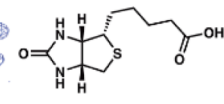
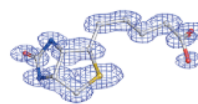
*acetaminophen, 2*



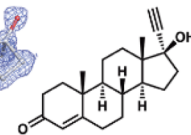
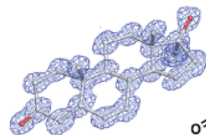
*ibuprofen, 3*



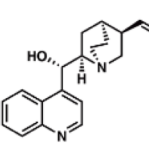
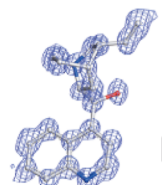
*carbamazepine, 4*



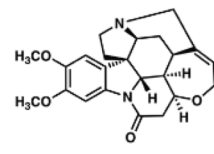
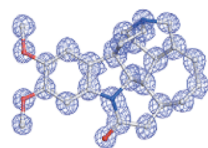
*biotin, 6*



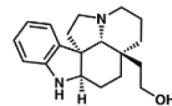
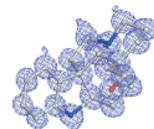
*ethisterone, 7*



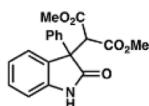
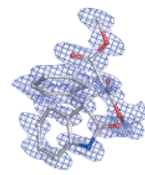
*cinchonine, 8*



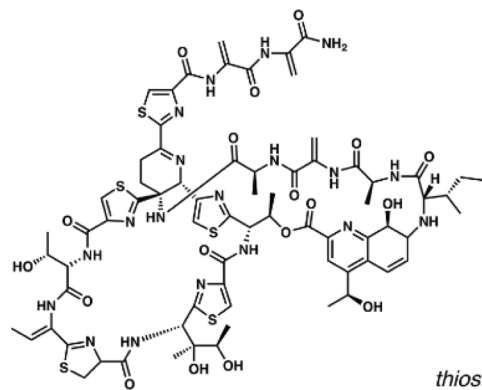
*brucine, 9*



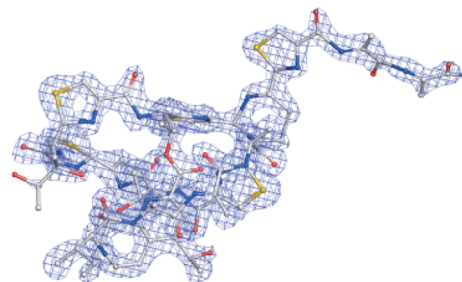
*synthetic (+)-  
limaspermidine, 10*



*synthetic oxindole,  
HKL-I-029, 11*



*thioestrepton, 5*





# Small Molecules: Flask to Structure

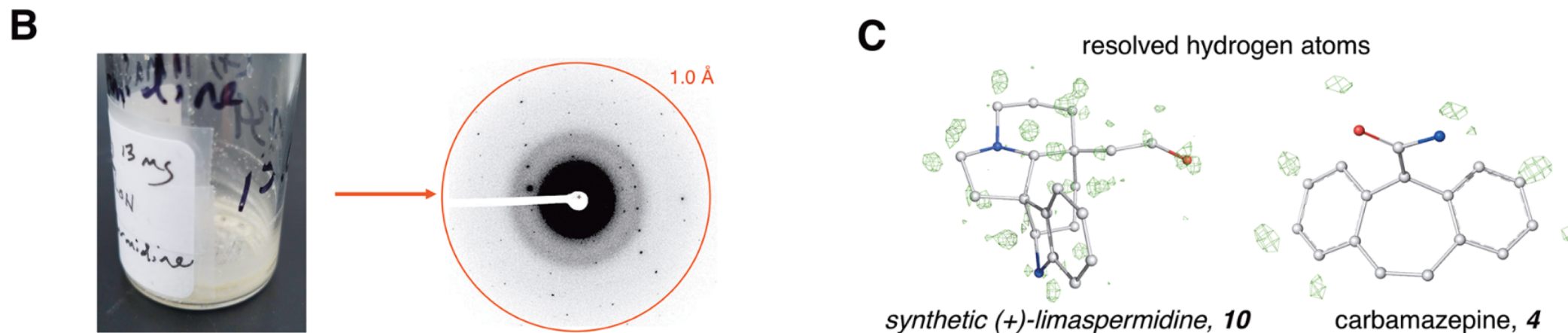


**Figure 2.** Different types of small molecules solved by MicroED. (A) Several pharmaceuticals, vitamins, commercial natural products, and synthetic samples resolved through MicroED. (B) Example of an amorphous film utilized in this study leading to 1 Å resolution data. (C) Protons could be observed for several compounds through MicroED. Green density are  $F_o - F_c$  maps showing positive density belonging to hydrogen atoms of the molecule.

# Future Directions

- Collection on lower end (non FEG) microscopes
- FIB milling possibly becoming more popular for thicker crystals
- Trying to make it work better on slower (non RS) cameras
  - Lack of continuous collection complicates processing
- Add parameters for MicroED to X-ray software



# Summary

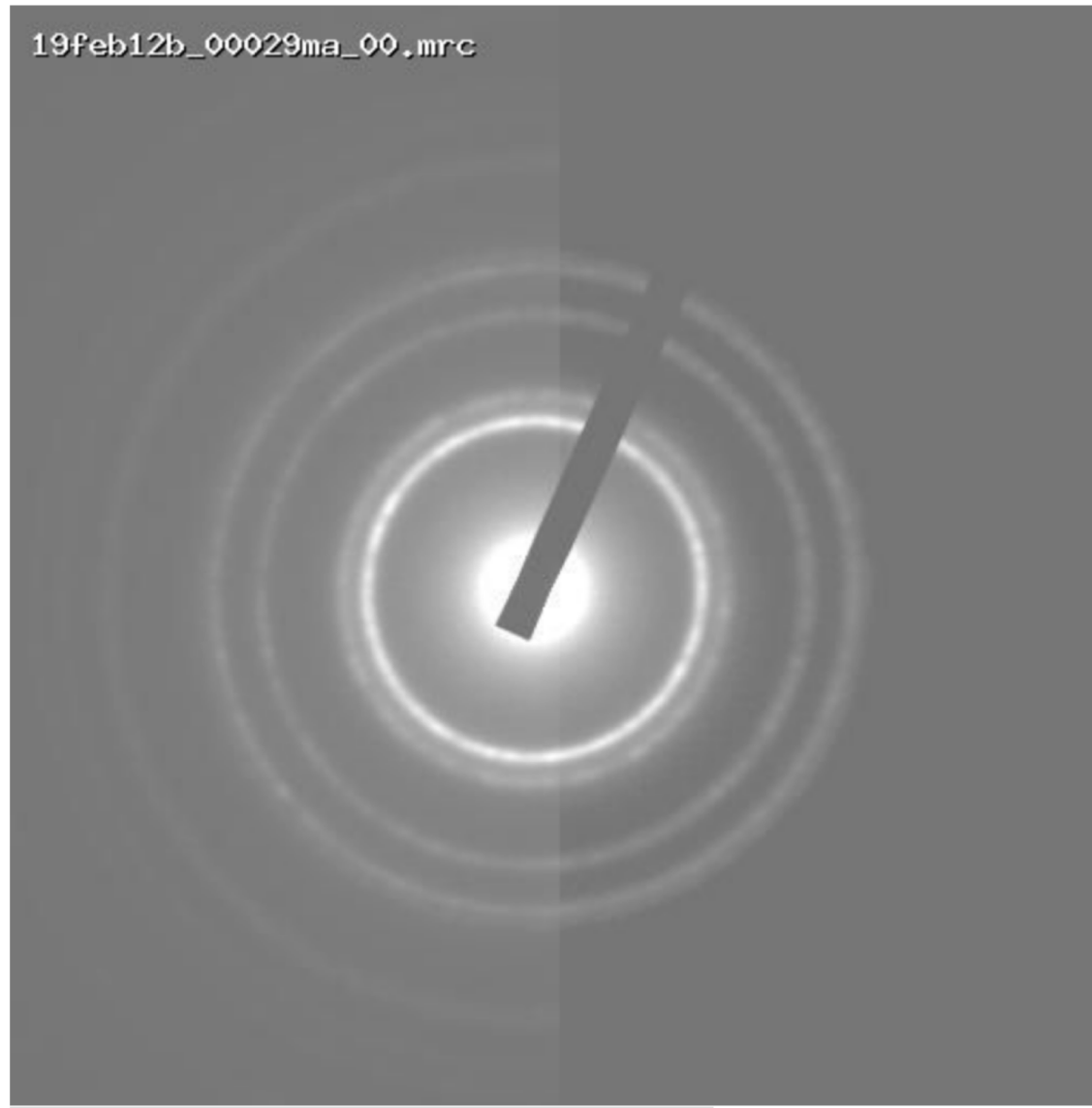
- Advantages

- Mid-level equipment (200 keV, FEG, CMOS detector with movie mode)
- Alignment probably less difficult than for imaging mode
- Highest resolution yet achieved by cryo-EM technique
- Processing software (X-ray) mature and well understood by a large community

- Disadvantages

- Crystals must be small (400 nm max thickness) and randomly oriented
  - FIB if necessary
- High quality stage essential, continuous slow tilting mode needed
- Phasing problem: molecular replacement needed for most protein structures

# Questions



Gold diffraction on J1230  
Outer ring: 1.2 Å resolution

# References

## References

[1-13]

1. Hattne, J., et al., *MicroED data collection and processing*. Acta Crystallogr A Found Adv, 2015. **71**(Pt 4): p. 353-60.
2. Iadanza, M.G. and T. Gonen, *A suite of software for processing MicroED data of extremely small protein crystals*. J Appl Crystallogr, 2014. **47**(Pt 3): p. 1140-1145.
3. Liu, S., et al., *Atomic resolution structure determination by the cryo-EM method MicroED*. Protein Sci, 2017. **26**(1): p. 8-15.
4. Nannenga, B.L. and T. Gonen, *Protein structure determination by MicroED*. Curr Opin Struct Biol, 2014. **27**: p. 24-31.
5. Nannenga, B.L., et al., *Structure of catalase determined by MicroED*. Elife, 2014. **3**: p. e03600.
6. Nannenga, B.L., et al., *High-resolution structure determination by continuous-rotation data collection in MicroED*. Nat Methods, 2014. **11**(9): p. 927-930.
7. Rodriguez, J.A., D.S. Eisenberg, and T. Gonen, *Taking the measure of MicroED*. Curr Opin Struct Biol, 2017. **46**: p. 79-86.
8. Rodriguez, J.A. and T. Gonen, *High-Resolution Macromolecular Structure Determination by MicroED, a cryo-EM Method*. Methods Enzymol, 2016. **579**: p. 369-92.
9. Rodriguez, J.A., et al., *Structure of the toxic core of alpha-synuclein from invisible crystals*. Nature, 2015. **525**(7570): p. 486-90.
10. Sawaya, M.R., et al., *Ab initio structure determination from prion nanocrystals at atomic resolution by MicroED*. Proc Natl Acad Sci U S A, 2016. **113**(40): p. 11232-11237.
11. Shi, D., et al., *The collection of MicroED data for macromolecular crystallography*. Nat Protoc, 2016. **11**(5): p. 895-904.
12. Shi, D., et al., *Three-dimensional electron crystallography of protein microcrystals*. Elife, 2013. **2**: p. e01345.
13. Yonekura, K., et al., *Electron crystallography of ultrathin 3D protein crystals: atomic model with charges*. Proc Natl Acad Sci U S A, 2015. **112**(11): p. 3368-73.